

The Copahue Volcanic-Hydrothermal System and Applications for Volcanic Surveillance

9

M. Agosto and J. Varekamp

Abstract

During the last two decades, Copahue and its active acidic crater lake have shown different magmatic, phreatomagmatic, and hydrothermal manifestations. Geochemical data of waters from Copahue springs, lakes and rivers provide new insights into the behavior of its volcano-hydrothermal system. Temporal variations in the chemical (major anions and cations) compositions, element fluxes, and isotopic fluctuations (δD and $\delta^{18}\text{O}$; stable Pb isotopes, $^{129}\text{I}/^{127}\text{I}$, $\delta^{37}\text{Cl}$, $\delta^7\text{Li}$, $\delta^{34}\text{S}$) of surface waters from Copahue for the period 1997–2012 can be related to processes in the underlying hydrothermal system. The 2000 and 2012 eruptive periods and the 2004 thermal anomaly showed increases in SO_4 , Cl and F contents in the waters as a result of ascending magmatic fluids. The changing chemical compositions also showed evidence for enhanced water/rock interaction during these magmatic periods, with increased concentrations of the major rock forming elements such as Al, K and Mg. Soon after the magmatic events, the elemental fluxes from the hydrothermal system decreased strongly, especially for K and Al. The latter is related to a decrease in permeability in the system through crystallization of alunite. Stable isotopic data (δD and $\delta^{18}\text{O}$) indicate that the hydrothermal fluids consist of a mixture of meteoric and magmatic waters that are affected by evaporation and water/rock interaction processes. The $\delta^7\text{Li}$ values, polythionate concentrations and water stable isotope ratios indicate that the hot spring

M. Agosto (✉)
GESVA-IDEAN (UBA-CONICET),
Dpto. Cs. Geológicas, FCEN,
Universidad de Buenos Aires,
Ciudad Universitaria, Pab.2,
1428 Buenos Aires, Argentina
e-mail: magusto@gl.fcen.uba.ar

J. Varekamp
Department of Earth and Environmental Sciences,
Wesleyan University, 265 Church Street,
Middletown, CT 06459-0139, USA

on the flank of the crater does not carry simple seepage from the crater lake. The crater lake and hot spring are fed by different sections from the underlying hydrothermal system. Temperatures of ~ 260 °C in the deeper part of the volcano-hydrothermal reservoir were estimated based on $\delta^{34}\text{S}$ values in sulfur and dissolved sulfate. The upper part of the system is possibly more dilute and cooler at ~ 175 °C, based on silica geothermometry. The presence of ^{129}I in the hydrothermal fluids indicates that subducted sediment with organic matter is one source for the magmatic volatiles. Stable Pb isotope ratios showed that the acidic hydrothermal fluids are dissolving local host rocks from the Copahue volcano edifice. The pyroclastic material ejected during the eruptive events carried the hydrothermal alteration phases silica, jarosite, alunite, and anhydrite/gypsum; liquid and particulate native sulfur was also emitted in large quantities. The chemical composition of the Upper Rio Agrio is controlled by the emissions of the feeding volcanic hot springs and mixing with glacial melt water. The compositional evolution of the large Lake Caviahue reflects inputs from the Upper Rio Agrio and melt water dilution, as well as mineral precipitation from the lake waters. The Lower Rio Agrio had copious amounts of Fe-sulfates in the river bed since 2003, which started to disappear again during the period of the 2012 eruption. Monitoring of SO_4/Cl , Mg/Cl and Al/Cl in the Upper Rio Agrio waters may constitute an efficient mode of volcanic surveillance, complementing the ongoing multidisciplinary volcano monitoring and forecasting at Copahue.

Keywords

Copahue volcano • Geochemistry of waters • Crater lake eruptions • Río Agrio • Volcano monitoring

9.1 Introduction

The chemical composition of volcanic fluids is of great interest to volcanologists because fluctuations in composition and elemental fluxes may aid in volcano activity monitoring. Extensive and detailed geochemical investigations of fluid discharges are part of many volcano geochemical monitoring programs (Stoibert and Rose 1970; Giggenbach 1987; Martini et al. 1991; Takano et al. 1994a, b; Vaselli et al. 2010). Many active volcanic systems have crater lakes, dependent on the local hydrology and climate (Pasternack and Varekamp 1997). They can be viewed as the uppermost manifestation of a hydrothermal

reservoir situated between the surface and the top of the underlying magma chamber. The physical-chemical features of a crater lake depend strongly on the inputs of magmatic-volcanic fluids apart from meteoric waters, so changes in lake chemistry can be interpreted in terms of precursors to pending volcanic activity. Moreover, crater lakes may also constitute a volcanic hazard because interaction between lake water and uprising magmas may produce phreatomagmatic or Surtseyan eruptions that can threaten the surrounding areas through ash fall-out and lahars (Healy et al. 1965; Brown et al. 1989; Cronin et al. 1997; Christenson 2000; Christenson et al. 2007, 2010). In addition, the large volumes of

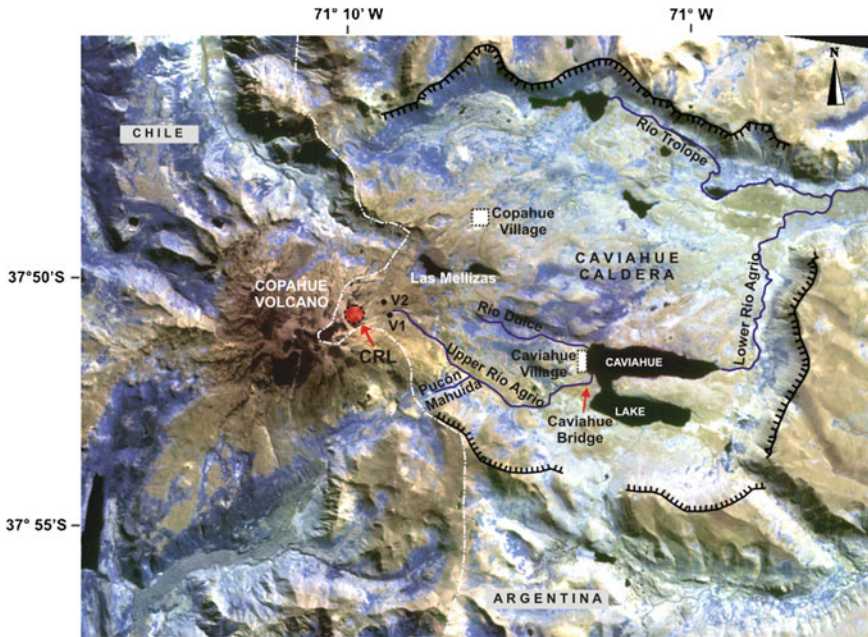


Fig. 9.1 Location map of Copahue volcano and sampling sites of the volcanic-hydrothermal manifestations (CRL, V1 and V2 hot springs), the hydrological system

(acid waters URA, CVL and LRA) and snowmelt waters (Río Dulce, Pucón Mahuida and Río Trolope)

toxic hot acid waters in crater lakes can become a danger if a retaining wall fails and lake expulsion and lahars may result, sending the hot and toxic fluids downhill into villages and rural lands. Many acid crater lakes are saturated with elemental sulfur, as indicated by floating sulfur spherules on the lake surface, and some of them have a pool of liquid sulfur at their bottom (Takano and Watanuki 1989; Takano et al. 1994a, b; Ohba et al. 2008). The sealing capacity of a molten sulfur pool at a lake bottom is a function of sulfur composition and temperature (Takano et al. 1994a, b; Kusakabe et al. 2000). Other minerals that may seal the lake bottom in ultra-acidic crater lakes are kaolinite, natroalunite, anhydrite, gypsum, pyrite, halite, barite, anglesite, celestite, amorphous silica, which may be expelled during phreatic eruptions (Christenson and Wood 1993; Delmelle and Bernard 1994; Varekamp et al. 2004; Christenson et al. 2010). The occurrence of a sealing zone may affect the mass and pressure of an injected, superheated vapor, and consequently, phreatic eruption modalities (Morrissey et al. 2010).

The Copahue active crater hosts a hot acidic lake, periodically with a floating sulfur slick, and several acidic hot springs (some below the summit glacier), which seep out from the eastern summit flank, and merge together downstream to form the Upper Río Agrio (Fig. 9.1). These features are the surface expressions of the volcanic-hydrothermal system of Copahue volcano; other hydrothermal areas around the volcano have geothermal pools and fumarolic emissions fed by a largely meteoric geothermal aquifer (Tassi et al. this book). This chapter deals with the variations in temperature and chemical composition of the Copahue crater lake (CRL), the flank thermal springs (called Vertientes, V), the Upper Río Agrio (URA), Lago Caviahue (CVL) and the Lower Río Agrio over the last 20 years as well as gas variations in elemental fluxes from the hot springs. The aim was to find relationships between these parameters and the ongoing volcanic activities of Copahue. All the available geochemical data for the magmatic-influenced waters were compiled and a conceptual model was proposed to explain

observed changes in the hydrological and geochemical regimes of the Copahue summit system over time. Strategies on how a safe and frequent monitoring program of the Upper Río Agrio were outlined to help to decipher possible variations in the summit magmatic-hydrothermal system within the context of volcanic surveillance.

9.2 Copahue Volcano: Hydrothermal Manifestations and Historical Activity

Copahue volcano hosts an acid brine-like crater lake (CRL) with a diameter of approximately 200 m (Fig. 9.2a). Acidic hot springs on the eastern flank, Vertiente 1 and 2 (V1 and V2), are located ~200 m below the crater rim and flow

into the Upper Río Agrio (URA) that discharges into Lago Caviahue (CVL), an acidified lake of glacial origin (Fig. 9.2b) (Varekamp et al. 2001, 2009; Gammons et al. 2005; Parker et al. 2008; Pedrozo et al. 2008; Varekamp 2008). Lago Caviahue has two arms and an outlet at the northern arm, the Lower Río Agrio (LRA), which joins the Río Trolope, which is largely meteoric water with some discharges from the geothermal system near Copahue village. The LRA exits the caldera in the NE corner and then passes through a large waterfall (Salto del Agrio) and then continues to merge 30 km further with the Río Ñorquén, and then goes further south towards Loncopué to ultimately discharge into the Río Neuquén (Gammons et al. 2005; Agosto et al. 2012). Representative tributaries to the acidic hydrological system are the Río Dulce (RD), Pucón Mahuida (PM) and Río Trolope

Fig. 9.2 a Photograph of Copahue crater lake, b Photograph taken from Copahue crater lake showing Vertientes (V1 and V2) hot springs, Upper Río Agrio and Lago Caviahue

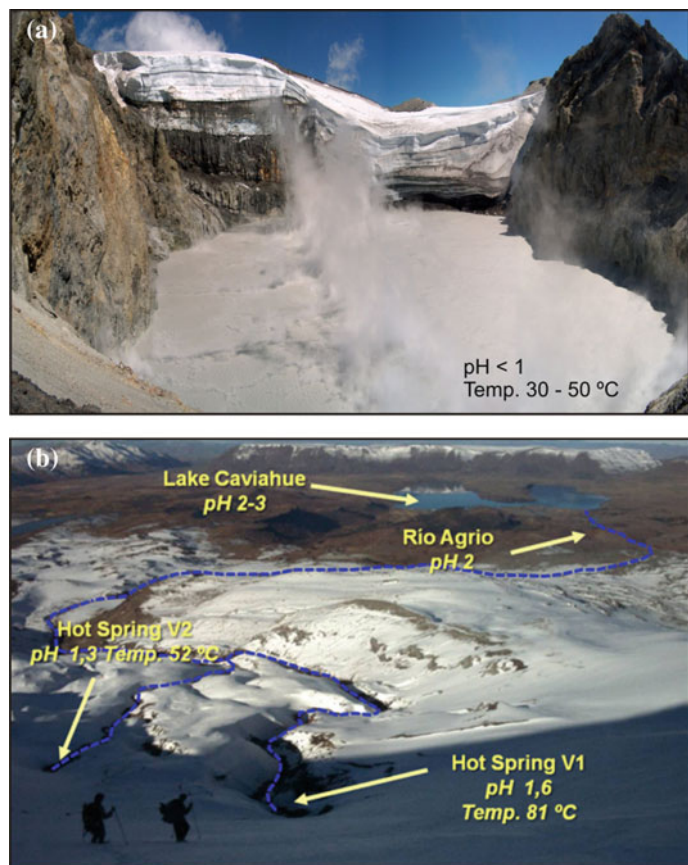


(Fig. 9.1). The area north-northeast of Copahue volcano hosts several hydrothermal emissions, which do not seem to be related to direct magmatic degassing, but are rather structurally controlled and fed by a separate, largely meteoric geothermal aquifer (Mas et al. 2000; Agosto et al. 2013a, b; Tassi et al. this book).

The recent activity of Copahue volcano involved a phreatic eruption cycle from the active crater that occurred from July 1992 to September 1995 (Delpino and Bermúdez 1993; Bermúdez and Delpino 1995). An initial phreatomagmatic eruption occurred in July 2000, followed by magmatic eruptions for several months (Delpino and Bermúdez 2002; Naranjo and Polanco 2004; Varekamp et al. 2001, 2004, 2009). The next phase of activity had the normally warm to hot (30–40 °C) crater lake surface become frozen from July to September 2004 (Caselli et al. 2005; Agosto 2011; Agosto et al. 2012), labeled here the 2004 negative thermal anomaly (NTA). The crater lake returned to its usual state in early 2005 and remained relatively constant until late 2011, when the discharge rate of fluids from the Copahue summit started to increase. During 2012 the crater lake water temperature increased and the water level decreased (Caselli et al. 2013; Agosto et al. 2013a), with a phreatic (phreatomagmatic?) event in July 2012, and finally a major phreatomagmatic-magmatic eruption that

took place in late December 2012 (Caselli et al. this book).

9.3 Analytical Data and Results

9.3.1 Temporal Evolution of the CRL, V1 and V2 Water Temperatures

The crater lake water temperature varied from 21 to 54 °C for the period 1997–2000, (Varekamp et al. 2001). A few months prior to the July 2000 eruption, the temperature of the crater lake water was extremely low: 8 °C in January and 5 °C in April 2000 (Pedrozo et al. 2008). Two years prior to the 2000 eruption hot spring temperatures were between 63–83 °C, and at 75 °C during the July 2000 events (Varekamp et al. 2001, 2004). No information on the lake water temperature is available for the period 2000–2003. In May 2004, the lake had a temperature of 13.5 °C with a gray-green color with sulfur patches floating on the lake surface (Fig. 9.3a). In July 2004, ~80 % of the lake surface was frozen (Fig. 9.3b) (Caselli et al. 2005; Agosto 2011; Agosto et al. 2012). The following months the frozen portion of the lake surface reduced to ~40 % (Fig. 9.3c). Freezing of an active crater lake is a rare feature, and was never reported before for the Copahue crater lake



Fig. 9.3 Photographs of the acid crater lake of Copahue volcano and changes of temperature from May 2004 to December 2005 (modified from Agosto et al. 2012)

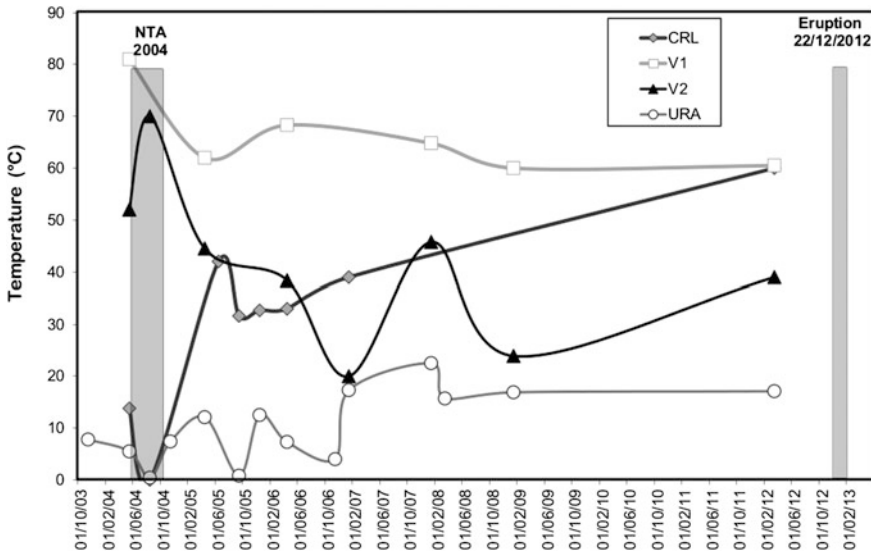


Fig. 9.4 Temporal variations in water temperatures from CRL, V1, V2 and URA

although the lake temperature before the 2000 eruption also approached the freezing point. The 2004 NTA was not followed by an eruption. During the crater lake NTA, the Vertientes hot springs showed the highest temperatures measured since 2003: 81 °C (V1) and 69 °C (V2). Afterwards, the V1 and V2 temperatures remained relatively constant ($T_{V1} = 60\text{--}70$ °C, and $T_{V2} = 40\text{--}50$ °C) (Agosto et al. 2012). The hot springs that feed the Upper Río Agrío do not affect the temperature of the river greatly because it is largely snowmelt water. The URA water temperature varies from 2 °C in winter to 13 °C in summer (Fig. 9.4). The crater lake and hot spring water temperatures are less sensitive to seasonal temperature changes than the URA (Fig. 9.4), whose waters receive large amounts of snow and ice melt water from tributary streams during southern spring-summer period (October-December) and small meteoric water inputs during the low rainfall of austral summer-autumn period (December-April). During 2004–2005 the weather was not anomalous at the region (AIC 2007), thus the 2004 lake NTA cannot be ascribed to climatic conditions. By the end of that year, the crater lake returned to its usual appearance (Fig. 9.3d), and during the following years (2005–2011) it had temperatures between 30 and 40 °C. During 2012 the crater lake temperature increased up to 63 °C in

March, and the water level decreased. Two weeks after a phreatic explosion event in July 2012 the temperature of CRL was similar to the previous measurement (60 °C) while the water level continued to fall (Agosto et al. 2013a). When the major phreatomagmatic eruptions occurred in December 2012 (Caselli et al. this book) the CRL diameter was reduced to approximately 20 m.

9.3.2 Chemical Composition of the Copahue Volcanic-Hydrothermal System

The CRL water is characterized by a low pH (<1–1.7), and specific conductivity up to 102 mS/cm. The crater lake has high contents of SO_4 , Cl and F, up to 66,000, 9,100, and 950 mg/L, respectively 7 months prior to the 2000 eruption, and up to 42,000, 18,000 and 2,000 mg/L respectively 8 months prior to the 2012 eruption. These contents are comparable to those of the hot springs V1 and V2 (concentrations of SO_4 , Cl and F up to 45,400, 6,800, and 500 mg/L, respectively prior to the 2000 eruption, and up to 28,000, 8,500 and 600 mg/L respectively prior to the 2012 eruption). The pH values of the V1 and V2 springs also range from <1 to 1–2. The specific conductivity of the URA waters decreases from 284 to 1.05 mS/cm from source to

the entrance of Lago Caviahue, as a result of the inputs of tributary streams that are largely fed by snowmelt (Agusto et al. 2012). These tributaries such as Pucón Mahuida have a higher pH and lower SC (pH = 6.3 and SC = 0.03 mS/cm). The Río Dulce stream is largely made of snowmelt water (pH = 6.65, SC = 0.01 mS/cm), and discharges into CVL, which has pH values that ranged over time from 2.2 to ~3 and relatively low SC (1.06 mS/cm). A similar decrease in the concentration of major and trace elements downstream in the URA was documented by earlier workers (Gammons et al. 2005; Ouimette 2000). The acidic hydrological system thus changes from hyperacidic (pH < 1–2) at the source to a pH between 2.55 and 3 in the CVL, and ultimately reaching a pH of 6 near Loncopué, after joining the Río Neuquén. Below CVL, the pH of the LRA remains near 3 until the confluence of the Río Trolope, below which point the pH rises and Fe-sulfates precipitated in abundance. The precipitation front of the sulfate mineral suite slowly moved from the confluence of the Río Trolope upstream in the LRA until it almost reached the outflow point of CVL in 2008–2009. Since 2012, the yellow brown precipitates have started to disappear and dissolve again.

Gammons et al. (2005) documented a similar spatial pattern of changes in water chemistry downstream in the LRA, with additional data on the concentration of major and trace elements, including the rare earth elements. The authors showed that the overall trends in Fe, Al and other rock-forming elements followed predicted patterns based on mineral solubilities, with precipitation of Fe-rich minerals occurring in the pH range 2.5–4, and precipitation of Al-bearing compounds in the pH range 4.5–6.

The CRL, V1, V2 and URA waters have a $\text{SO}_4(\text{Cl})\text{-Ca}(\text{Fe}, \text{Al})$ composition, whereas CVL waters are $\text{SO}_4/\text{Cl}\text{-Na}(\text{Mg}, \text{Ca})$ type. The RD water has a $\text{HCO}_3\text{-Ca}$ composition, whereas PM water shows a $\text{SO}_4\text{-Ca}$ composition that is different with respect to the typical meteoric water likely due to the influence of the volcanic ash plumes from Copahue volcano (Agusto 2011). Waters from the system (CRL, V1, V2 and URA)

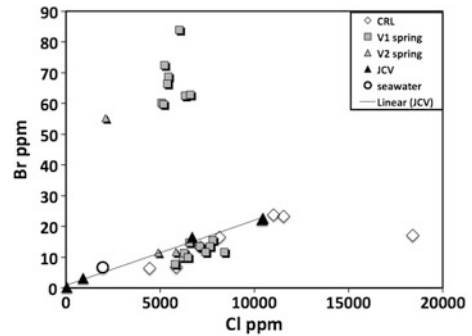


Fig. 9.5 Cl–Br data from V and CRL and CVL

have $\Sigma\text{anions}/\text{salinity}$ molar ratios of 0.8–0.9, and $\Sigma\text{cations}/\text{salinity}$ molar ratios of 0.1–0.2, where anions are SO_4 , Cl, F, Br and cations Na, K, Al, Ca, Fe and Mg. The total anion content (hereafter TAC) is thus a good approximation for the total salinity. The S/Cl values range from 1 to 9 and Br/Cl values show bimodal distribution (Fig. 9.5). Br/Cl ratios scatter shows an upper cluster and a lower linear trend, the high Br values are in V1 fluids and one high value in V2, while all the CRL values plot on the linear trend with seawater Br/Cl. High Br values in V1 and V2 are related with a period of TAC increment (see below).

The volcanic elements (VE) derive from the input of magmatic gases into the hydrothermal cell with condensation and recirculation of the fluids between the degassing magma and the shallow zone. Magmatic gases such as CO_2 , SO_2 , HCl and HF (and minor volatile elements such as As, Hg and B) are absorbed into the hydrothermal cell by scrubbing processes (Symonds et al. 2001) acidifying the waters of the system, except for the CO_2 which may escape into the geothermal aquifer. The condensation of the magmatic water in the hydrothermal cell creates a mixture of glacial melt water that seeped into the super structure of the mountain and magmatic water. The rock forming elements (RFE) derive from water rock interaction between the very hot and acid fluids and the volcanic rocks at depth. At temperatures >200 °C and pH values near zero, rock dissolution is probably near congruent, although some minerals may dissolve faster than

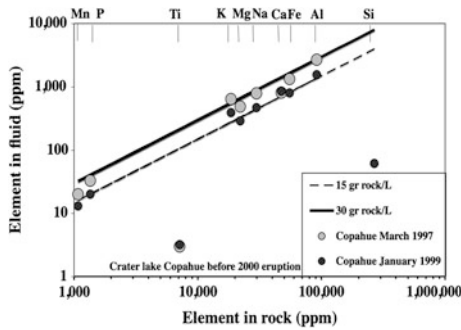


Fig. 9.6 Isosol diagram with 15 and 30 g isosols and CRL compositions in 1997 and 1999. The off sets of Ti and S indicate retention of these two elements in the reservoir (or for Ti also precipitation in the lake). The distance Si–Si* is the amount of Si retained (8 g silica per 15 g rock dissolved)

others. A simple way to express the element relations for near congruent rock dissolution is the isosol diagram (Varekamp 2015), which shows the element concentrations in the rock protoliths versus the same elements in the fluids. The isosols are lines of equal dissolution (grams rock/liter fluid), and an example is given for crater lake fluids of 1997 and 1999 (Fig. 9.6). The diagram indicates 30 g rock dissolved/liter in 1997 and 15 g/L in 1999. In the lake, this drop in rock contents can be simply the result of dilution with glacial melt water. Both patterns show strong depletions in Ti and Si, indicating that either Ti is not completely dissolved from the source rocks or precipitated in the lake through a Ti-rich mineral. The silica was never completely dissolved in the hydrothermal fluids and precipitated while rock dissolution was ongoing (Varekamp 2015). The amount of hydrothermal silica retained by the system can be calculated from the isosol value minus the observed Si value (the vertical intercept on Fig. 9.6 for Si), which for the 1999 fluids is 4000 ppm Si expected and 61 ppm Si observed. This implies that with 15 g rock dissolved per liter, 8 g of hydrothermal silica are retained in the system.

Speciation saturation calculations on the V and CRL fluids indicate that hydrothermal silica, anhydrite and possibly some Cu sulfides are almost always saturated in the fluids (Varekamp et al. 2001, 2009). During some periods the fluids

became more concentrated and jarosite and alunite were predicted to be stable phases (Quimette 2000; Varekamp et al. 2004, 2009; Fazio et al. 2008). These potential relationships can be documented in molar triangular diagrams such as Na-5 K-Mg with the minerals olivine, albite and alunite indicated (Fig. 9.7a). The bulk rock composition (2000 basaltic andesite of Copahue, Varekamp et al. 2004) is shown and most fluid compositions cluster around this andesitic rock index point (ARIP). Many compositions plot away from the alunite pole, indicating crystallization of that phase, whereas some fluid compositions plot towards the alunite phase, suggesting redissolution in the fluids of older alunite deposits. The diagrams with Fe-Ca-Na+K (Fig. 9.7b) and Mg-Na+K-Al (Fig. 9.7c) show similar relations for crystallization of anhydrite, jarosite and alunite. There are no fluid compositions trending towards albite-plagioclase suggesting no preferential dissolution of that mineral, but a few data points lay towards early dissolution of olivine (Mg enrichment in fluids). In summary, the volcanic-hydrothermal system underlying Copahue active crater consists of glacial meltwater that is acidified by magmatic gases. That mixture dissolves the host rock near congruently, while silica and anhydrite precipitate and at certain periods jarosite and alunite crystallize. The crystallization of the latter phases and the occurrence of liquid native sulfur may lead to reduced permeability in the system, as discussed below. The V fluids discharge into the URA and then afterward are released into Lake Caviahue, to be discussed in detail later.

9.3.3 Isotope Compositions

9.3.3.1 δD and $\delta^{18}O$ of Water

The stable isotope compositions of water in term of δD and $\delta^{18}O$ are a good tracer for hydrological processes such as mixing of magmatic waters with meteoric waters and evaporation. The springs, rivers and lakes at Copahue show a wide range of isotopic compositions, ranging from pure meteoric waters to highly evolved waters with high values of δD and $\delta^{18}O$ (Table 9.1, after

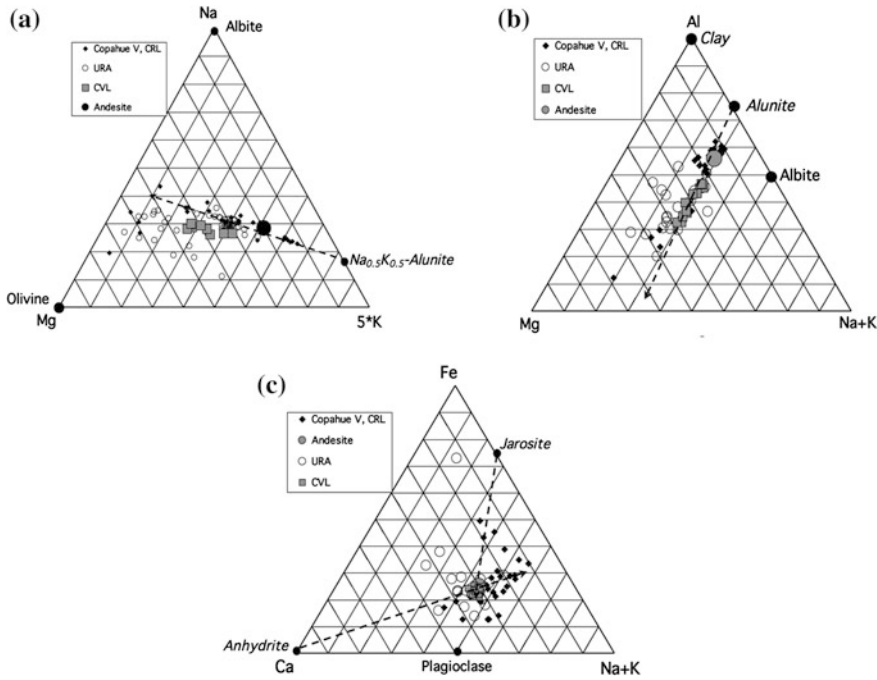


Fig. 9.7 Molar triangular diagrams: **a** Al-Mg-Na+K, showing the ARIP and the tail of water compositions in V and CRL that indicate alunite crystallization; **b** Fe-Ca-Na +K, showing the ARIP and anhydrite crystallization; **c** Na-Mg-5 K, showing evidence for alunite crystallization and a slight offset between the V and URA compositions

Quimette 2000; Varekamp et al. 2001, 2004; Agosto 2011). The $\delta^{18}\text{O}$ values for acidic waters ranged between -12.1 and -5.9 ‰ V-SMOW, and δD values between -90 and -22.5 ‰ V-SMOW (URA and CRL, respectively). Snowmelt waters (PM and RD) show the lowest isotopic values, with $\delta^{18}\text{O}$ values ranging between -10.8 and -12.1 ‰ V-SMOW, and δD values between -77 and -88 ‰ V-SMOW; these are the meteoric end member waters for this volcanic-hydrothermal system.

The $\delta^{18}\text{O}$ - δD diagram (Fig. 9.8a) shows the Local Meteoric Water Line (LMWL: $\delta\text{D} \text{‰} = 7.8 * \delta^{18}\text{O} \text{‰} - 0.21 \text{‰}$), based on data from the regional precipitation network in Mendoza. The LMWL differs slightly from the global meteoric water line (Craig 1961), which is the result of local atmospheric fractionation processes. The OIPC web site (Bowen and Revenaugh 2003) provides values for local meteoric water at Caviahue and Copahue (OIPC-<http://www.waterisotopes.org>), in good agreement with

the empirical LMWL (Caviahue: $\delta\text{D} = -70 \text{‰}$, $\delta^{18}\text{O} = -9.9 \text{‰}$; Copahue summit: $\delta\text{D} = -90 \text{‰}$, $\delta^{18}\text{O} = -12.6 \text{‰}$). Local meteoric water (Table 9.1) plot on a line with the equation $\delta\text{D} \text{‰} = 4.95 * \delta^{18}\text{O} \text{‰} - 26.32 \text{‰}$ (Fig. 9.8b) which include data from meteoric water ponds that show extreme evaporation (pond near airport of Caviahue and the Laguna Auquinco (Lat -37.357486 ; Long -69.992266 , elev. 1400 m) in the desert near Chos Malal. This line shows the effects of evaporation of pure meteoric waters at mean ambient temperatures (about $11 \text{ }^\circ\text{C}$) and local relative humidity (60 %). The intersection of the evaporation line and LMWL gives a value similar to the OIPC value for mean LMW in Caviahue and close to those defined by Panarello (2002) ($-80 \pm 5 \text{‰}$ for δD , and $-11.2 \pm 0.4 \text{‰}$ for $\delta^{18}\text{O}$). Andesitic waters (AW), as defined by Taran et al. (1989) and Gigenbach and Corrales Soto (1992), have $\delta^{18}\text{O}$ and δD values of $+10 \pm 3 \text{‰}$ and $-20 \pm 10 \text{‰}$, respectively. The CRL and V water samples plot on a line with

Table 9.1 Temperatures (°C), pH and Specific Conductivity (SC, mS/cm) values, chemical (mg/L) and isotopic ($\delta^{18}\text{O}$ and δD , ‰ V-SMOW) composition from regional waters

Sampling Point	Date	Reference	T °C	pH	SC	HCO_3^-	SO_4^-	Cl^-	F^-	Br^-	Na	K	Ca	Mg	Fe	Si	Al	δD	$\delta^{18}\text{O}$
<i>Crater Lake (CRL)</i>																			
	3/15/1997	1	54*	0.3	n.a	n.a	64200	10300	960	n.a	790	640	810	490	1320	n.a	2700	-26	3.6
	3/20/1998	1	33*	0.3	n.a	n.a	59600	8600	840	n.a	590	480	800	370	960	n.a	2020	-36	1.5
	1/6/1999	1	21*	0.3	n.a	n.a	55400	8000	720	n.a	470	390	850	290	800	n.a	1560	-37	0.4
	11/26/1999	1	33*	0.2	n.a	n.a	66000	9100	950	n.a	430	370	840	270	750	n.a	1490	-30	3.5
	1/17/2001	1	n.a	1.1	n.a	n.a	20000	4300	230	n.a	460	50	450	1830	1780	n.a	360	-54.6	-3.3
	3/21/2002	1	n.a	0.6	n.a	n.a	34900	9000	740	n.a	700	80	680	1430	2100	n.a	1040	n.a	n.a
	1/18/2003	1	n.a	0.6	n.a	n.a	31700	14500	970	n.a	1200	260	1020	1470	1890	n.a	2400	-22.5	5.9
	5/5/2004	2	14	0.8	n.a	n.a	9590	3805	423	n.a	280	79	419	296	262	n.a	416	-62.6	-6
	8/20/2004	2	0?	0.6	n.a	n.a	11915	4385	249	n.a	609	178	375	324	337	41	585	n.a	n.a
	11/23/2004	1	n.a	0.8	n.a	n.a	20700	6700	520	n.a	560	170	900	590	760	n.a	1190	n.a	n.a
	4/13/2005	2	n.a	n.a	n.a	n.a	8875	6498	1134	n.a	417	201	715	311	292	64	817	-48.6	-2
	6/13/2005	2	42	n.a	n.a	n.a	9903	6668	768	n.a	366	188	745	282	355	84	914	n.a	n.a
	9/15/2005	2	32	0.8	60500	n.a	10127	7164	864	n.a	290	181	636	232	327	101	878	n.a	n.a
	12/6/2005	2	33	0.4	101500	n.a	17134	7486	932	n.a	364	246	570	232	313	64	451	n.a	n.a
	4/8/2006	2	33	0.6	65200	n.a	17326	7135	568	13	1006	186	834	397	314	61	566	n.a	n.a
	1/29/2007	2	39	1.7	9500	n.a	22476	8145	625	16	422	202	689	293	n.a	n.a	n.a	n.a	n.a
	11/30/2007	2	n.a	n.a	n.a	n.a	32016	11012	766	24	399	242	802	276	n.a	n.a	n.a	n.a	n.a
	12/11/2007	2	n.a	n.a	n.a	n.a	33003	11552	851	23	448	275	898	321	n.a	n.a	n.a	n.a	n.a
	3/14/2008	2	n.a	n.a	n.a	n.a	18980	5874	450	7	227	163	565	207	n.a	n.a	n.a	n.a	n.a
	3/18/2009	3	n.a	n.a	n.a	nd	12873	4442	407	6	177	104	368	127	n.a	n.a	n.a	n.a	n.a
	3/6/2012	3	63	<0	n.a	n.a	41748	18404	1917	17	84	36	143	98	619	n.a	n.a	n.a	n.a

(continued)

Table 9.1 (continued)

Sampling Point	Date	Reference	T °C	pH	SC	HCO ₃ ⁻	SO ₄ ⁻	Cl ⁻	F ⁻	Br ⁻	Na	K	Ca	Mg	Fe	Si	Al	δD	δ ¹⁸ O
<i>Hot Spring (V)</i>																			
	3/15/1997	1	68*	0.4	n.a	n.a	64200	10600	nd	n.a	940	790	1100	640	2190	n.a	3870	-33	1.9
	3/20/1998	1	63*	0.4	n.a	n.a	64000	10200	nd	n.a	1020	930	1420	640	2270	n.a	3690	-38	0.9
	1/6/1999	1	83*	0.3	n.a	n.a	65400	9800	700	n.a	910	880	770	500	1860	n.a	3250	-33	1.7
	11/26/1999	1	72*	0.2	n.a	n.a	45400	6800	500	n.a	520	470	800	300	970	n.a	1940	-49	-2.1
	7/16/2000	1	75*	0.8	n.a	n.a	51400	8400	700	n.a	1500	710	610	1870	2780	n.a	5320	-33.4	1.1
	1/17/2001	1	n.a	2.4	n.a	n.a	30900	4300	230	n.a	900	660	710	960	1580	n.a	2950	-76.3	-9.8
	3/21/2002	1	n.a	1.5	n.a	n.a	24500	7800	1300	n.a	1180	190	860	2830	3590	n.a	1720	-48.9	-2.4
	1/18/2003	1	n.a	1.7	n.a	n.a	11100	6600	750	n.a	1010	60	600	1870	2140	n.a	1010	n.a	n.a
	3/14/2004	1	n.a	2.3	n.a	n.a	15600	9800	840	n.a	1540	130	680	1720	2610	n.a	2210	n.a	n.a
	11/23/2004	1	n.a	1.5	n.a	n.a	8800	3800	220	n.a	540	120	630	640	780	n.a	1020	n.a	n.a
<i>Hot Spring (V1)</i>																			
	2/25/2004	2	n.a	n.a	n.a	n.a	2746	2192	287	n.a	245	34	203	405	367	n.a	443	n.a	n.a
	1/15/2004	2	n.a	n.a	n.a	n.a	2190	1747	246	n.a	73	9	89	120	135	n.a	126	-46	-1.4
	5/5/2004	2	81	1.6	n.a	n.a	14995	2140	441	n.a	1562	225	989	703	495	n.d	1492	-52.5	-3.8
	4/13/2005	2	62	1.4	n.a	n.a	11988	7026	524	n.a	759	263	735	814	672	49	1510	n.a	n.a
	4/8/2006	2	68	0.9	28400	n.a	12236	5025	419	n.a	950	262	516	814	765	39	911	n.a	n.a
	1/29/2007	2	n.a	n.a	n.a	n.a	14587	4929	406	n.a	981	214	589	599	n.a	n.a	n.a	n.a	n.a
	5/31/2007	2	n.a	n.a	n.a	n.a	20050	7107	357	14	1035	322	803	819	n.a	n.a	n.a	n.a	n.a
	11/30/2007	2	n.a	n.a	n.a	n.a	19643	5798	290	8	792	377	736	602	n.a	n.a	n.a	n.a	n.a
	12/11/2007	2	n.a	n.a	n.a	n.a	20687	6211	314	10	851	416	800	599	n.a	n.a	n.a	n.a	n.a
	12/15/2007	2	n.a	n.a	n.a	n.a	20887	6280	294	11	828	403	762	583	n.a	n.a	n.a	n.a	n.a
	1/5/2008	2	n.a	n.a	n.a	n.a	21651	6477	309	10	893	446	794	601	n.a	n.a	n.a	n.a	n.a
	1/12/2008	2	65	1.7	33500	n.a	21538	6558	306	15	787	445	755	572	n.a	n.a	n.a	n.a	n.a
	2/12/2008	2	n.a	n.a	n.a	n.a	25703	7804	307	16	1006	537	735	677	n.a	n.a	n.a	n.a	n.a

(continued)

Table 9.1 (continued)

Sampling Point	Date	Reference	T °C	pH	SC	HCO ₃ ⁻	SO ₄ ⁻	Cl ⁻	F ⁻	Br ⁻	Na	K	Ca	Mg	Fe	Si	Al	δD	δ ¹⁸ O
	3/2/2008	2	n.a	n.a	n.a	n.a	25757	7651	326	14	1011	525	748	722	n.a	n.a	n.a	n.a	n.a
	3/11/2008	2	n.a	n.a	n.a	n.a	26084	7424	317	12	1028	535	741	823	n.a	n.a	n.a	n.a	n.a
	12/7/2008	2	n.a	n.a	n.a	n.a	18748	5065	146	60	587	359	764	462	n.a	n.a	n.a	n.a	n.a
	12/9/2008	2	n.a	n.a	n.a	n.a	19218	5182	78	60	616	380	791	475	n.a	n.a	n.a	n.a	n.a
	1/2/2009	2	n.a	n.a	n.a	n.a	21905	6326	153	63	706	430	742	495	n.a	n.a	n.a	n.a	n.a
	1/22/2009	2	60	0.8	32200	n.a	22700	6598	221	63	753	456	738	511	n.a	n.a	n.a	n.a	n.a
	29/02/10	4	n.a	n.a	n.a	n.a	16880	5218	470	72	591	408	825	390	n.a	n.a	n.a	n.a	n.a
	3/9/2010	4	n.a	n.a	n.a	n.a	19798	5427	502	69	611	411	766	399	n.a	n.a	n.a	n.a	n.a
	3/18/2010	4	n.a	n.a	n.a	n.a	20598	6010	590	84	783	447	745	529	n.a	n.a	n.a	n.a	n.a
	3/31/2010	4	n.a	n.a	n.a	n.a	19512	5384	493	66	611	993	763	407	n.a	n.a	n.a	n.a	n.a
	3/6/2012	3	60.5	0.6	n.a	n.a	27934	8411	594	12	820	587	826	549	770	n.a	n.a	n.a	n.a
<i>Hot Spring (V2)</i>																			
	5/5/2004	2	52	1.3	n.a	n.a	16260	1825	139	n.a	1010	161	985	628	485	n.a	1141	n.a	n.a
	8/20/2004	2	70	1.4	n.a	n.a	20590	8283	232	n.a	997	211	720	1469	678	n.a	1991	n.a	n.a
	4/13/2005	2	45	1.5	n.a	n.a	9700	5341	375	n.a	537	171	670	622	653	40	1123	-62.6	-6.1
	4/8/2006	2	38	1.5	23800	n.a	18085	7468	604	n.a	769	129	587	588	480	27	689	n.a	n.a
	1/29/2007	2	20	2.3	21200	n.a	5701	1641	169	n.a	219	72	181	252	n.a	n.a	n.a	n.a	n.a
	1/12/2008	2	46	1.7	23700	n.a	15158	4901	272	12	630	267	634	474	n.a	n.a	n.a	n.a	n.a
	1/22/2009	2	24	1.1	39000	n.a	6688	2113	114	55	232	99	318	204	n.a	n.a	n.a	n.a	n.a
	3/6/2012	3	39	1.2	n.a	n.a	19234	5848	381	12	550	343	712	420	585	n.a	n.a	n.a	n.a
<i>Upper Río Agrio (URA)</i>																			
	1/7/1999	1	n.a	n.a	n.a	n.a	4740	950	46	n.a	100	65	170	100	170	36	280	-64	-7.2
	11/25/1999	1	n.a	n.a	n.a	n.a	1060	180	15	n.a	24	14	49	25	31	15	55	-54	-3.3
	7/6/2000	1	n.a	n.a	n.a	n.a	1220	130	21	n.a	33	7	88	130	130	n.a	76	-85.2	-11.5
	1/13/2001	1	n.a	n.a	n.a	n.a	790	120	11	n.a	27	9	72	58	34	23	45	-76.6	-10.3

(continued)

Table 9.1 (continued)

Sampling Point	Date	Reference	T °C	pH	SC	HCO ₃ ⁻	SO ₄ ⁻	Cl ⁻	F ⁻	Br ⁻	Na	K	Ca	Mg	Fe	Si	Al	δD	δ ¹⁸ O
	3/24/2002	1	n.a	n.a	n.a	n.a	1170	280	36	n.a	26	5	45	71	53	19	44	-80.8	-10.8
	1/21/2003	1	n.a	n.a	n.a	n.a	460	170	17	n.a	30	6	44	62	23	20	27	-82.8	-11.6
	11/6/2003	2	8	2.4	1560	n.a	n.a	n.a	n.a	n.a	29	5	47	48	n.d	27	102	n.a	n.a
	1/15/2004	2	n.a	3	n.a	n.a	585	457	57	n.a	51	6	79	93	74	n.a	81	n.a	n.a
	1/25/2004	2	n.a	3	n.a	n.a	737	594	70	n.a	66	6	89	120	96	n.a	111	n.a	n.a
	2/24/2004	2	n.a	2	n.a	n.a	1438	1135	123	n.a	131	22	160	247	219	n.a	236	n.a	n.a
	3/12/2004	1	n.a	n.a	n.a	n.a	2790	1490	120	n.a	210	34	160	310	320	n.a	260	n.a	n.a
	5/5/2004	2	6	2	n.a	n.a	1604	614	57	n.a	88	15	161	152	137	n.d	123	n.a	n.a
	8/20/2004	2	0	2.3	n.a	n.a	1720	890	30	n.a	40	15	79	103	617	n.a	136	n.a	n.a
	11/12/2004	2	7	2.4	n.a	n.a	598	238	15	1.3	29	10	58	49	50	n.a	59	n.a	n.a
	11/22/2004	1	n.a	n.a	n.a	n.a	560	180	11	n.a	28	6	36	40	32	n.a	41	n.a	n.a
	4/13/2005	2	12	2	n.a	n.a	1977	1067	70	n.a	122	35	166	153	170	23	230	-83.3	-10.8
	9/15/2005	2	1	2.2	5100	n.a	799	437	38	n.a	49	17	56	59	79	16	106	n.a	n.a
	12/6/2005	2	13	2.7	1438	n.a	391	123	11	n.a	6	10	22	22	23	9	29	n.a	n.a
	4/8/2006	2	7	2.5	9685	n.a	2255	834	90	n.a	116	41	153	108	121	17	164	n.a	n.a
	11/14/2006	2	4	2.7	1975	n.a	490	174	14	0.3	9	4	33	31	36	n.a	42	-86.4	-11.9
	1/29/2007	2	17	2.7	3420	n.a	983	312	23	n.a	54	13	68	62	n.a	n.a	n.a	-89.6	-11.2
	11/12/2007	2	30	2.5	5370	n.a	1109	344	25	0.6	53	19	69	56	n.a	n.a	n.a	n.a	n.a
	11/19/2007	2	n.a	n.a	n.a	n.a	994	303	26	0.5	51	18	71	56	n.a	n.a	n.a	n.a	n.a
	11/28/2007	2	n.a	n.a	n.a	n.a	692	202	21	0.3	32	12	43	34	n.a	n.a	n.a	n.a	n.a
	12/27/2007	2	n.a	n.a	n.a	n.a	1303	388	28	0.6	62	24	82	67	n.a	n.a	n.a	n.a	n.a
	1/13/2008	2	23	2.7	7200	n.a	2342	696	58	1.3	103	42	137	104	n.a	n.a	n.a	n.a	n.a
	1/27/2008	2	n.a	n.a	n.a	n.a	2229	655	54	1.2	99	39	128	101	n.a	n.a	n.a	n.a	n.a
	2/10/2008	2	n.a	n.a	n.a	n.a	2711	791	59	1.5	116	49	147	116	n.a	n.a	n.a	n.a	n.a
	2/19/2008	2	n.a	n.a	n.a	n.a	3463	979	96	2	137	60	168	130	n.a	n.a	n.a	n.a	n.a

(continued)

Table 9.1 (continued)

Sampling Point	Date	Reference	T °C	pH	SC	HCO ₃ ⁻	SO ₄ ⁻	Cl ⁻	F ⁻	Br ⁻	Na	K	Ca	Mg	Fe	Si	Al	δD	δ ¹⁸ O
	3/2/2008	2	n.a	n.a	n.a	n.a	4496	1239	95	2.5	n.a	n.a	n.a	n.a	n.a	n.a	n.a	n.a	n.a
	3/16/2008	2	16	1.5	23760	n.a	6656	1794	176	6.7	250	114	285	240	n.a	n.a	n.a	n.a	n.a
	4/30/2008	2	n.a	n.a	n.a	n.a	4670	1342	186	2.4	184	86	236	201	n.a	n.a	n.a	n.a	n.a
	5/4/2008	2	n.a	n.a	n.a	n.a	5840	1637	127	4.2	218	101	283	227	n.a	n.a	n.a	n.a	n.a
	6/24/2008	2	n.a	n.a	n.a	n.a	1513	443	73	0.8	55	26	92	57	n.a	n.a	n.a	n.a	n.a
	7/20/2008	2	n.a	n.a	n.a	n.a	6266	1744	121	3.2	62	29	103	67	n.a	n.a	n.a	n.a	n.a
	7/27/2008	2	n.a	n.a	n.a	n.a	1752	493	74	0.9	64	29	104	69	n.a	n.a	n.a	n.a	n.a
	8/8/2008	2	n.a	n.a	n.a	n.a	844	232	21	0.4	31	15	53	34	n.a	n.a	n.a	n.a	n.a
	8/26/2008	2	n.a	n.a	n.a	n.a	1790	496	73	1	62	27	102	68	n.a	n.a	n.a	n.a	n.a
	9/9/2008	2	n.a	n.a	n.a	n.a	863	232	21	0.4	31	14	51	34	n.a	n.a	n.a	n.a	n.a
	9/23/2008	2	n.a	n.a	n.a	n.a	861	229	21	0.4	32	15	53	35	n.a	n.a	n.a	n.a	n.a
	9/30/2008	2	n.a	n.a	n.a	n.a	861	230	21	0.4	31	15	53	35	n.a	n.a	n.a	n.a	n.a
	10/7/2008	2	n.a	n.a	n.a	n.a	874	231	21	0.4	31	14	52	34	n.a	n.a	n.a	n.a	n.a
	12/29/2008	2	n.a	n.a	n.a	n.a	1138	321	17	3.6	43	19	73	52	n.a	n.a	n.a	n.a	n.a
	1/17/2009	2	17	1.9	10140	n.a	2271	633	29	4.2	80	37	130	97	n.a	n.a	n.a	n.a	n.a
	3/6/2012	3	17	1.4	n.a	n.a	2394	689	44	1.4	84	36	143	98	75	n.a	n.a	n.a	n.a
<i>Lake Caviahue (CVL)</i>																			
	19/03/1998 N	1	n.a	2.3	n.a	n.a	370	85	nd	n.a	13	7	20	14	18	n.a	29	n.a	n.a
	06/07/2000 S	1	n.a	2.2	n.a	n.a	480	104	9	n.a	12	8	22	14	19	n.a	26	-76.3	-10
	11/6/2003	2	15	2.2	980	n.a	n.a	n.a	n.a	n.a	8	4	19	12	nd	24	45	n.a	n.a
	5/5/2004	2	11	2.4	n.a	n.a	n.a	n.a	n.a	n.a	8	7	49	22	16	nd	14	-81	-10.8
	8/20/2004	2	5	2.9	n.a	n.a	n.a	n.a	n.a	n.a	nd	6	15	18	20	n.a	17	n.a	n.a
	11/12/2004	2	9	3.1	n.a	n.a	n.a	n.a	n.a	n.a	8	5	30	16	19	n.a	17	n.a	n.a
	21/11/2004 N	1	n.a	2.6	n.a	n.a	330	80	8	n.a	15	5	20	22	22	n.a	22	n.a	n.a
	4/13/2005	2	12	2.8	n.a	n.a	260	91	13	n.a	15	9	17	17	24	13	22	n.a	n.a

(continued)

Table 9.1 (continued)

Sampling Point	Date	Reference	T °C	pH	SC	HCO ₃ ⁻	SO ₄ ⁻	Cl ⁻	F ⁻	Br ⁻	Na	K	Ca	Mg	Fe	Si	Al	δD	δ ¹⁸ O
	9/15/2005	2	6	2.9	1050	n.a	178	60	9	n.a	3	9	9	12	19	13	16	-82.2	-10.2
	12/6/2005	2	9	2.6	1344	n.a	305	70	9	n.a	n.d	7	8	14	18	7	15	n.a	n.a
	4/8/2006	2	12	3.0	1205	n.a	326	77	5	0.1	10	14	23	17	18	8	15	n.a	n.a
	11/14/2006	2	9	2.8	1110	n.a	225	59	6	n.a	13	4	18	20	15	n.a	12	-88	-10.7
	14/11/06 S	2	10	3.2	930	n.a	186	52	5	n.a	10	3	14	16	6	n.a	10	-82.1	-11.1
	14/11/06 N	2	7	3.1	1060	n.a	229	65	6	n.a	12	4	18	19	16	n.a	14	n.a	n.a
	2/7/2007	2	12	3.1	n.a	n.a	314	66	6	n.a	12	4	18	20	n.a	n.a	n.a	n.a	n.a
	11/12/2007	2	9	2.8	1110	n.a	317	76	5	0.1	13	4	19	18	n.a	n.a	n.a	n.a	n.a
	1/17/2009	2	15	2.9	1260	n.a	277	76	4	1.6	14	5	20	18	n.a	n.a	n.a	n.a	n.a
<i>Lower Río Agrio (LRA)</i>																			
Puente NE	11/14/2006	2	10	3.1	1050	n.a	218	60	5	0.06	11	4	17	18	17	n.a	12	n.a	n.a
Salto del Agrio	11/14/2006	2	12	3.5	380	n.a	85	23	2	0.05	7	2	11	9	5	n.a	5	-86.7	-11.7
Puerta de Trolope	11/14/2006	2	13	3.6	330	n.a	83	23	2	0.02	5	2	9	7	2	n.a	4	n.a	n.a
Puente - Río Ñorquin	11/14/2006	2	13	3.7	240	n.a	73	20	2	0.03	5	2	13	7	n.a	n.a	3	n.a	n.a
Loncopue	11/14/2006	2	14	6.7	110	13	34	9	1	0.01	1	2	11	5	n.a	n.a	n.a	n.a	n.a
<i>Snowmelt waters</i>																			
Río Dulce (RD)	11/14/2006	2	4	6.7	10	9	4	0.8	2	n.a	0.6	1	1	0.1	n.a	n.a	n.a	-84.6	-11
Las Mellizas	11/14/2006	2	1	6.3	290	7	44	11	0.5	0.015	7	2	10	9	n.a	n.a	n.a	n.a	n.a
Hualcupen	11/14/2006	2	12	7	10	15	0.8	0.4	0.1	0.002	2	0.8	2	1	n.a	n.a	n.a	-88.39	-12.08
Pucón Mahuida (PM)	11/14/2006	2	5	6.3	30	4	12	1	0.2	n.d	2	1	2	2	n.a	n.a	n.a	n.a	n.a
Río Trolope	11/14/2006	2	11	6.2	30	17	8	2	0.1	0.004	3	1	3	2	n.a	n.a	n.a	-86.7	-11.7

n.a not analyzed. Reference data: * Varekamp et al. (2001), (1) Varekamp et al. (2009), (2) Augusto et al. (2013a), (3) Augusto et al. (2013a), (4) this work

a lesser slope that trends towards the AW field (Fig. 9.8a), labeled here the VHS line (volcano-hydrothermal system) with the equation $\delta D \text{ ‰} = 3.6 * \delta^{18}O \text{ ‰} - 41.65 \text{ ‰}$. The VHS line intersects with the LMWL roughly at the same point as the meteoric water evaporation line. The slope of evaporation lines is defined by:

$$S = [h^*(\delta_{\text{atm}} - \delta_w) + \varepsilon]D / [h^*(\delta_{\text{atm}} - \delta_w) + \varepsilon]^{18}O \quad (9.1)$$

where the ε parameters are the total fractionation factors for a given h^* and temperature, δ_w are the isotopic values of the waters that are evaporating and δ_{atm} are the isotopic values of atmospheric moisture (Gat 1995). The latter can be taken as in equilibrium with the precipitation at the ambient temperature or can be approximated from an empirical relationship with ambient temperature, which was done here (Gibson et al. 1999). The common relative humidity h is applicable for waters at similar temperature as the atmosphere, but for waters well above ambient temperatures, h^* is the water temperature-normalized relative humidity, defined as $(P_w(\text{atm}) \text{ at } T_{\text{atm}} \text{ at } h) / (P_w(\text{water}) \text{ at } T_{\text{water}} \text{ at saturation})$ (Gat 1995; Varekamp and Kreulen 2000). The slope of the meteoric water evaporation line of 4.95 can be obtained from the above equation at a mean annual ambient temperature of 11 °C and $h \sim 0.6$. The VHS line is largely the result of mixing between meteoric and magmatic/andesitic waters (V fluids), with the CRL fluids having an additional evaporation component. Some fluids from the geothermal system also plot near the VHS line, which is the result of evaporation at an elevated temperature (Varekamp and Kreulen 2000), not the result of mixing with andesitic fluids. The V fluids are most likely binary mixtures between magmatic fluids (“andesitic waters” or AW) and glacial melt water, and this would suggest that the V fluids may consist of >50 % of magmatic fluids (Varekamp et al. 2004), with a range over time based on our total data from highs of 70 % to extreme lows of 10 %. The low % values occurred during and after eruptive activity, thus

the enhanced W/R interaction during intrusive/extrusive events likely led to a reduced permeability in the upper part of the system as a result of mineral precipitation. That led to a diminished rise of the deep hydrothermal fluids and as a result the effluents at the Vertientes springs and feeders into the crater lake became more dilute. These mixing calculations for the V fluids assume that the glacial melt waters mix with pure magmatic fluids, but the W/R interaction will also add ^{18}O to the mix (no 2H because rocks are poor in hydrogen). Average rock consists of about 45 % (wt) of oxygen, and the V waters have up to 10 % TDS. A simple calculation for congruent dissolution of 10 % rock yields $\sim 4.5 \text{ ‰}$ of oxygen with $\delta^{18}O = +8 \text{ ‰}$, which would make the V water possibly 1 % heavier in $\delta^{18}O$ than simple binary mixing of meteoric/glacial water and andesitic water. The composition of the CRL is most likely a combination of mixing between a hydrothermal component from the underlying reservoir and glacial meltwater, with simultaneous evaporation. The geothermal pools in the geothermal/fumarolic areas around the volcano edifice seem to be largely steam-heated waters close to meteoric in origin and the evaporation effect dominates there, (e.g., Panarello 2002; Agosto 2011; Tassi et al. this book). The slope of the line for the geothermal samples (about coincident with the VHS line) indicates that evaporation occurred at about 30 °C, which is the typical low-end range temperature of the crater lake and the typical temperature of the geothermal pools. The effects of mixing and evaporation can be further separated for the CRL samples, in a Cl versus $\delta^{18}O$ plot, where the Cl contents are less strongly influenced by evaporation than the $\delta^{18}O$ values. The CRL values plot on a line, which is a combined mixing-evaporation line (Varekamp and Kreulen 2000). The V samples plot on a simple mixing line for the more concentrated samples but show more scatter in the more dilute V compositions. The latter are the result of the temporal changes in the hydrothermal reservoir that led to variations in Cl concentration and $\delta^{18}O$ values (Fig. 9.8c). The evaporation of warm CRL waters would be accompanied by HCl

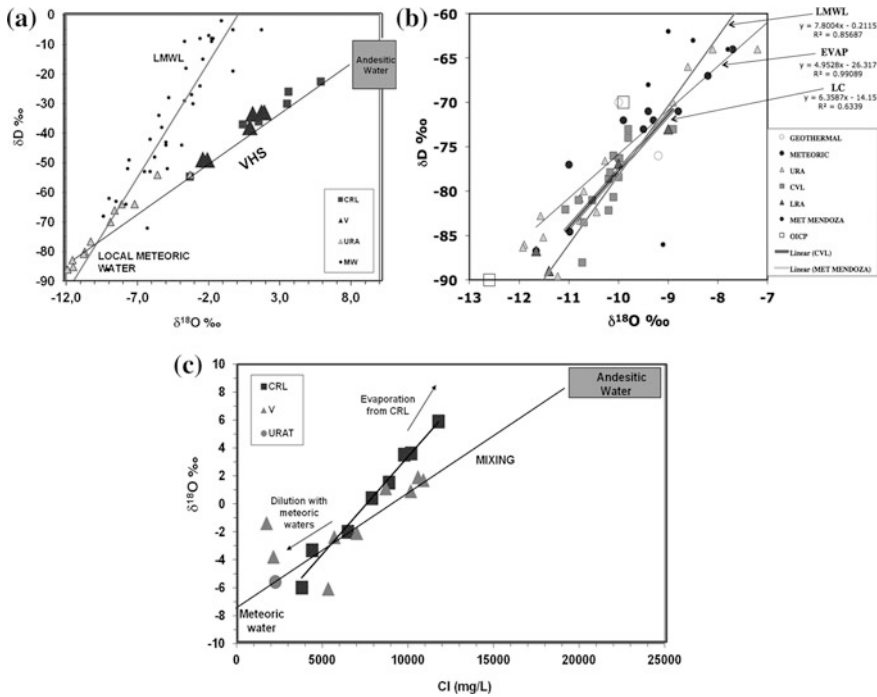


Fig. 9.8 Stable isotopes of water: **a** a. $\delta^{18}O$ — δD diagram with CRL, V fluids on mixing line and URA fluids near meteoric water. Also indicate the LMWL; **b** URA-CVL-LRA and MW data, showing the range of values in CVL as a result of both in situ precipitation

(Geothermal and Meteoric data from Varekamp et al. 2004); **c** mixing and evaporation for CRL and V samples in Cl- $\delta^{18}O$ diagram. Note the evaporation line for CRL samples

escape, while the evaporation of water would concentrate the Cl^- . More detailed data are needed to model quantitatively the combined water and HCl evasion from the lake.

The Upper Rio Agrio and Lago Caviahue samples are all close to the meteoric water end-member but in detail the effects of mixing (URA) and evaporation (CVL) can be detected (Fig. 9.8b). The E/I value (Evaporation over Input; Gat and Levy 1978) for Lago Caviahue was calculated from the CVL isotope data array and the meteoric water endmember, using the same evaporation parameters as that for the meteoric water evaporation line (see also Mayr et al. 2007). This provides a range of $E/I = 4-6\%$, indicating that evaporation is only a small component in the CVL water balance. The range of isotope values for CVL (-88 to -73% for δD) can be explained as follows: glacial melt water has a δD of -87% and theoretical

precipitation at the summit of Copahue (~ 3000 m elevation) has a δD of -90% (OIPC). Observed URA water with the lightest composition has $\delta D -89.6\%$. This water enters the lake and mixes with the lake fluids and the isotopically lightest lake values are -88% . The CVL array of data points ends near -73% , which is also close to the theoretical mean value for precipitation around Caviahue (1600 m elevation, OICP). Mixing between those meteoric endmember values as well as evaporation creates the array of isotope data for CVL with a slope of 6.4, which as a result of the evaporation component is slightly less than the slope of the pure LMWL of 7.8.

The URA has up to 8% magmatic water in its higher reaches, which then decreases downstream because of dilution of the Vertiente spring waters with glacial melt waters. The geothermal fluids from the pipe from the geothermal drill

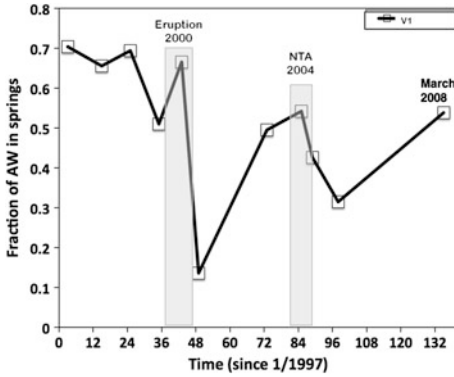


Fig. 9.9 Mixing diagram of AW versus MW in V fluids versus time. Note the two drop off events after the 2000 eruption and the 2004 NTA

hole show an offset to heavier $\delta^{18}\text{O}$ from LMW (more details Tassi et al. this book), typical for non-magmatic hydrothermal systems (Craig et al. 1963).

The V waters can provide the closest estimate of the isotopic composition of the volcano-hydrothermal reservoir fluids, which consist for >50 % of magmatic fluids (AW). The time trend of the AW % in the V fluids shows a strong decrease after the 2000 eruption and after the 2004 NTA (Fig. 9.9), indicating the decrease in the flux of deep hydrothermal fluids to the surface as a result of the reduced permeability in the system. The freezing of the crater lake at that

time was a direct result of the decreased input of hot deep hydrothermal waters into the lake.

In summary, the V fluids are binary mixtures between magmatic fluids and meteoric waters, whereas the other mineralized waters are impacted by mixing with V type fluids and evaporation processes, be it at ambient or at slightly elevated temperatures. The fluids from the pools in Copahue village and the geothermal steam pipe stem from the geothermal aquifer are dominated by meteoric water. That system on the north flank of the mountain seems to be spatially well-separated from the acid volcano-magmatic hydrothermal system that occurs directly below the Copahue summit and its crater lake.

9.3.3.2 $\delta^{34}\text{S}$ and Sulfur Speciation

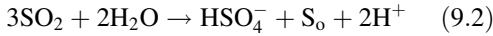
The sulfur isotopic composition of fluids at Copahue has been measured in several samples at different times. The $\delta^{34}\text{S}$ for dissolved sulfate in V, CRL, URA, CVL and elemental sulfur samples from the slicks on the crater lake, from the crater lake wall as well as from the crater lake sediment were collected and analyzed (Table 9.2). In general, the $\delta^{34}\text{S}$ in bisulfate or sulfate is rather high, ranging from +13.7 to +21.2 ‰ over time. The elemental sulfur is much lighter, ranging from -8.2 to -11.4 ‰. The difference in $\delta^{34}\text{S}$ between the oxidized and

Table 9.2 Sulfur isotope data and $\delta^{18}\text{O}$ (‰) in sulfate

Sampling point	1993	1995	1997	1999	2000	2001	2002	2003
CRL	n.a.	n.a.	14.2	14.2	n.a.	13.6	16.6	21.2
V	n.a.	n.a.	14.5	14.2	15	14.8	18.3	14.8
URA-P	n.a.	n.a.	14.4	13.9	14.3	n.a.	n.a.	n.a.
URA-D	n.a.	n.a.	14.1	n.a.	14	n.a.	n.a.	n.a.
CVL	n.a.	n.a.	14.1	13.7	14.3	n.a.	n.a.	n.a.
CVL	n.a.	n.a.	14	n.a.	14.4	n.a.	n.a.	n.a.
URAT	n.a.	n.a.	n.a.	14	n.a.	n.a.	n.a.	n.a.
S ^o	-10.5	-11.4	n.a.	-8.2	-10.9	n.a.	n.a.	n.a.
S in sediment	-8.4	n.a.	n.a.	n.a.	n.a.	n.a.	n.a.	n.a.
$\Delta\delta^{34}\text{S}$ V	n.a.	n.a.	24.5	24.2	25	24.8	28.3	24.8
XII $\delta^{18}\text{O}$ -SO ₄	n.a.	n.a.	20.6	19.6	16.8	n.a.	n.a.	n.a.
XII $\delta^{18}\text{O}$ -H ₂ O	n.a.	n.a.	1.9	1.7	1.1	n.a.	n.a.	n.a.

n.a not analyzed

reduced sulfur species is created during the disproportionation of SO_2 in water according to:



The isotopic fractionation is determined by temperature and in the lower temperature range also by the kinetics of the process (Kusakabe et al. 2000). The calculated temperatures of the $\delta^{34}\text{S}$ system for the hydrothermal system range from 250–280 °C (Varekamp et al. 2004) assuming that the native sulfur stems from the deep reservoir. The copious amounts of liquid sulfur ejected during phreatic events in the 1990s and 2012 eruption (Delpino and Bermudez 1993; Agosto et al. 2013a) indicates that the hydrothermal system contains a vast reservoir of liquid sulfur that may escape with the fluids into the lake. The $\delta^{34}\text{S}$ in dissolved sulfate decreases downstream in the URA and CVL, although the effect is close to the data precision. This may be caused by the oxidation of reduced sulfur species in the water during its flow down the mountain, precipitation of sulfates along the way, or mixing with tributaries with isotopically lighter sulfur. More data are needed to establish the exact reason, but the trend is consistent over the years.

The $\delta^{18}\text{O}$ in sulfate is a tracer for the origin of the sulfate oxygen when it formed from less oxidized sulfur species (Boschetti 2013). At high temperature, magmatic SO_2 reacts with water to form HSO_4 (Eq. 9.2), and the $\delta^{18}\text{O}$ of the water and temperature determine the $\delta^{18}\text{O}$ value in sulfate. This value will reset rapidly during cooling and dilution at relatively high temperatures and low pH values, but it will be “frozen in” at ambient temperatures. Equilibration temperatures can be calculated for the hot spring using the $\delta^{18}\text{O}$ of the water and the $\delta^{18}\text{O}$ in bisulfate (Table 9.2). Using the expressions of Seal et al. (2000), temperatures of 93, 99, and 117 °C were obtained for the years 1997, 1999 and 2000. The $\delta^{18}\text{O}$ of the acid reservoir fluids is a mixture of water close to magmatic values (+8 ‰) and glacial melt water (−11 ‰) and the hot springs provide fluids of various mixtures between the two. An extreme endmember temperature can be calculated assuming that the

lowest section of the volcanic-hydrothermal reservoir was at the magmatic $\delta^{18}\text{O}$ value of +8 ‰, yielding an equilibration temperature of 183 °C, still well below the ~260 °C calculated earlier from sulfur isotope equilibrium considerations. Most likely, the waters have re-equilibrated during cooling and dilution with glacial melt water in the subsurface, and the obtained range of temperatures is close to the exit temperature of the V hot spring in these years (see Table 9.1). The temperatures calculated from the sulfur isotope fractionation (250–270 °C) probably provide the closest estimate to the true temperature of the magmatic fluid reservoir feeding the hyperacid crater lake and hot springs. These temperature estimations are similar to those based on gas chemical equilibria for the hydrothermal reservoir feeding fumarolic areas north-eastern of the volcano (Tassi et al. this book), and consistent with those measured in the geothermal wells (~260 °C) located near these areas (Mas et al. this book).

In 1996, 1997 and 2004, polythionate species were analyzed both in the crater lake waters and in the Vertientes hot spring (Table 9.2). The concentrations in 1996 and 1997 were very low compared to those documented in other acid volcanic lakes (Takano and Watanuki 1989; Takano et al. 1994a; Kusakabe et al. 2000; Delmelle and Bernard 2000a, b), whereas much higher concentrations were found in late 2004. Polythionate levels in the V springs were always below detection. The latter suggests that the CRL and V fluids draw from different parts of the underlying hydrothermal fluids, or alternatively, the CRL fluids have an active SO_2 input and the polythionates are generated within the lake environment. Either way, it is obvious from these data as well differences in cation ratios and stable isotope ratios between CRL and V fluids, that the V fluids are not direct seepage from the crater lake but have a source at depth independent of the crater lake fluids. The 2004 polythionate data show an order of magnitude higher polythionate concentrations than the late 1990s data, which has been interpreted at other lakes as an indicator of pending eruptions (Takano and Watanuki 1989). The November 2004 sampling of the

crater lake took place after the 2004 NTA, and hydrothermal input into the lake had been restored by that time. Possibly, SO₂ rich vapors were again entering the lake at that time, related to the input of deep magmatic fluids or even a small magmatic intrusion earlier that year (“failed eruption” of Varekamp et al. 2009; Velez et al. 2011; Augusto et al. 2012).

9.3.3.3 Stable Pb Isotope Ratios, ¹²⁹I, ³⁶Cl, $\delta^{37}\text{Cl}$, and $\delta^7\text{Li}$

Some more exotic isotope ratios and their elemental values were also analyzed in the Copahue acidic waters: ¹²⁹I, $\delta^7\text{Li}$, ³⁶Cl and stable Pb isotopes, be it that the number of analyses is very limited (Table 9.3). The isotope ¹²⁹Iodine is cosmogenic with a T_{1/2} = 16.5 Ma. Upon rain-out from the atmosphere into the ocean, the iodine gets largely incorporated into organic matter and then ends up in marine sediment. With its long half life time, it survives the subduction process and may then be released again during sediment devolatilization in the arc-magma generation zone. As such, the isotope is like ¹⁰Be one of the “smoking guns” of sediment subduction (Fehn et al. 2002). Nuclear industry contamination and weapons testing has raised the modern levels of ¹²⁹I above cosmogenic background levels, which needs to be considered in systems open to the atmosphere such as volcanic lakes. Measurements of ¹²⁹I were reported for CRL, V and CVL as well as local non-volcanic lakes (Fehn et al.

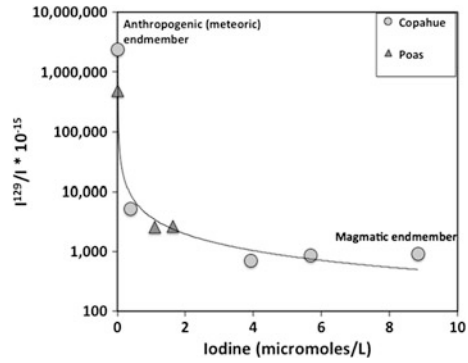


Fig. 9.10 Mixing diagram for magmatic fluids (I = 15 mmol, and ¹²⁹I/I = versus meteoric fluids (I = 0.00015 mmol and ¹²⁹I/I = 12,450,000 × 10⁻¹⁵), CRL, URA and V fluids from Copahue indicates as well as some crater lake fluids from Póas crater lake (after Fehn et al. 2002)

2002). Mixing curves of I versus ¹²⁹I/¹²⁷I show that the V and CRL fluids have excess amounts of ¹²⁹I (Fig. 9.10), suggesting the presence of a volatile component derived from degassing of subducted sediments in the magmatic fluids. The mixing curve is based on a magmatic endmember with 15 micromolar iodine and ¹²⁹I/I ratio of 700 10⁻¹⁵. Some data from Poas crater lake in Costa Rica are shown for comparison, which shows potentially a very similar magmatic endmember (Fehn et al. 2002). Crustal contamination with organic-rich sediments was assumed to not occur and that these are “deep” signals. The presence of a volatile component derived from subducted

Table 9.3 I, Cl and Br concentrations (mg/L) in Copahue fluids and $\delta^7\text{Li}$, $\delta^{37}\text{Cl}$ (‰) and Iodine and Pb isotope ratios

Sampling point	Date	I	Cl	Br	$\delta^7\text{Li}$	$\delta^{37}\text{Cl}$	²⁰⁷ Pb/ ²⁰⁶ Pb	²⁰⁸ Pb/ ²⁰⁶ Pb	¹²⁹ I/I × 10 ⁻¹⁵
URA	1997	0.04826	911	3.1	n.a.	+0.5	n.a.	n.a.	5160 ± 380
CVL	1997	0.007366	55	0.2	n.a.	+0.3	n.a.	n.a.	n.a.
CRL	1997	0.49784	10412	22.2	+8.4	+0.5	n.a.	n.a.	701 ± 59
V	1997	n.a.	n.a.		+3.4	+0.4	n.a.	n.a.	n.a.
CRL	1999	112,141	6695	16.5	n.a.	n.a.	0.8394	20,692	921 ± 49
V	1999	0.72009	10462	22.7	n.a.	n.a.	0.8390	20,702	860 ± 90
Lago Verde	1999	0.000152	n.a.	n.a.	n.a.	n.a.	n.a.	n.a.	2367580 ± 1320050
Pool V	1999	n.a.	n.a.	n.a.	n.a.	+0.7	n.a.	n.a.	n.a.

n.a not analyzed

organic material was also suggested by Agosto et al. (2013b) based on the measurements of $\delta^{13}\text{C-CO}_2$ and $\delta^{15}\text{N-N}_2$ in fumarolic gas samples from geothermal areas of Copahue (Tassi et al. this book).

The isotope ^{36}Cl also forms in the upper atmosphere, but its half-life is too short to survive the subduction process. However, it also forms during the spontaneous fissioning of U and Th isotopes (Fehn et al. 1992). Subducted sediment rich in U and Th thus has the potential to generate ^{36}Cl during the subduction process that is then released in the arc magma generation zone. If the transfer from mantle wedge to magma reservoir and magmatic degassing is not too long (several 1000 years at most), one can expect an inventory of ^{36}Cl in these magmatic fluids. The ^{36}Cl data in the Copahue crater lake and V fluids were relatively low (3 ± 3) and no clear constraints on magma residence time can be derived from these data.

The two $\delta^7\text{Li}$ values for the crater lake and V fluids, sampled in 1997, are +8.4 ‰ and +3.4 ‰, respectively (referenced to NIST 8545). Most arc rocks have $\delta^7\text{Li}$ values at 4 ± 1.5 (White 2013). During W/R interaction, ^7Li is preferentially removed from the rock matrix, creating higher $\delta^7\text{Li}$ values in the fluid relative to the protolith. The value in the CRL fluids is higher than the mean value in arc rocks, and thus may suggest a less complete degree of rock digestion below the lake. The V fluids may stem from a part of the hydrothermal system where more complete rock digestion takes place. Other explanations are possible as well, such as digestion of rocks that have undergone earlier W/R interaction which would constitute a Li-poor but ^6Li -enriched protolith. Most importantly, these isotopes confirm the earlier data on sulfur speciation that the crater lake and the hot springs draw fluids from spatially diverse sections of the overall hydrothermal system.

The stable Pb isotopes ^{206}Pb , ^{207}Pb and ^{208}Pb were measured in fluids from the crater lake and V spring (1999 samples). The two samples have comparable values for the ratios $^{207}\text{Pb}/^{206}\text{Pb}$ and $^{208}\text{Pb}/^{206}\text{Pb}$ (Table 9.3; ^{204}Pb was not measured with the ICP-MS because of interference of

^{204}Hg), which are also very close to these ratios in rock sample COP3 (2000 eruption cinders, Varekamp et al. 2006). These data show beyond any doubt that the volcanic-hydrothermal fluids below Copahue summit are dissolving and reacting with lava flows and pyroclastic rocks from Copahue volcano. The Pb isotope ratio in the Caviahue rock series is different (Varekamp et al. 2006), which makes those less likely protoliths for the fluids.

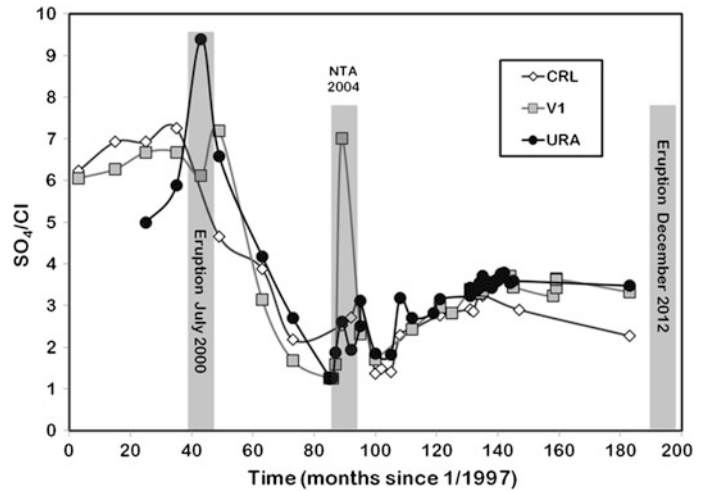
Stable Cl isotopes were measured in several samples (Table 9.3), and these $\delta^{37}\text{Cl}/^{35}\text{Cl}$ show small positive deviations from 0 (referenced to the seawater standard), ranging from +0.3 to +0.7 ‰. Most subducted sediments have small negative stable chlorine isotope values (Sharp et al. 2007; Barnes et al. 2009). Chlorine isotope fractionations occur during fluid—gas partitioning (Liebscher et al. 2006; Sharp et al. 2007) and the acid hydrothermal fluids may have lost some HCl that escaped into the hydrothermal aquifers in the flanks of the volcano, leaving the acid fluids slightly enriched in ^{37}Cl . Alternatively, the degassing of HCl from the magma may have fractionated the isotopes, leading to a ^{37}Cl enriched component in the hydrothermal fluids; volcanic gas samples from many other volcanoes show slightly positive values as well (Eggenkamp et al. 1994). The +0.5 ‰ value for the CRL sample may also be related to the observed loss of HCl vapors from the lake favored by the elevated temperature and salinity and the extremely low pH of lake waters (Rouwet and Ohba 2015).

9.4 Temporal Variations in Fluid Chemical Compositions

9.4.1 Variations in Chemistry of Copahue Crater Lake, Vertientes Hot Springs and Upper Río Agrio

The erupted products of the period 1992–2000, (Delpino and Bermudez 1993; Varekamp et al. 2001) showed the presence of hydrothermal silica and liquid native sulfur on the lake floor and

Fig. 9.11 Temporal variations of SO_4/Cl ratios in CRL, V and URA. Note the increase values during 2000 eruption and NTA 2004



probably in the underlying system as well. Varekamp et al. (2004) suggested that the saturation indices of the fluid system became more complex during the 2000 eruptive period, with a larger number of saturated mineral phases that included alunite. Vertientes hot springs and crater lake RFE compositions before the 2000 eruptions show low pH values with high concentrations of Al, K, Ca, Ti and P. These elements drop significantly in concentration after the 2000 eruptions; the pH values rose in the V fluids, whereas the CRL remained very acidic. The Mg and Mn concentrations increased during and after the eruptions (Varekamp et al. 2001), whereas the Fe concentrations show no clear time trends. During the July 2000 eruption of Copahue, an increase of Salinity/Cl by mass was associated with a marked increase in the relative proportion of SO_4 with respect to Cl (Fig. 9.11). After the eruptive period, the relative values of the more soluble species Cl and F gradually increased with respect to SO_4 (Varekamp et al. 2009) consistent with the newly injected degassing magma in the system.

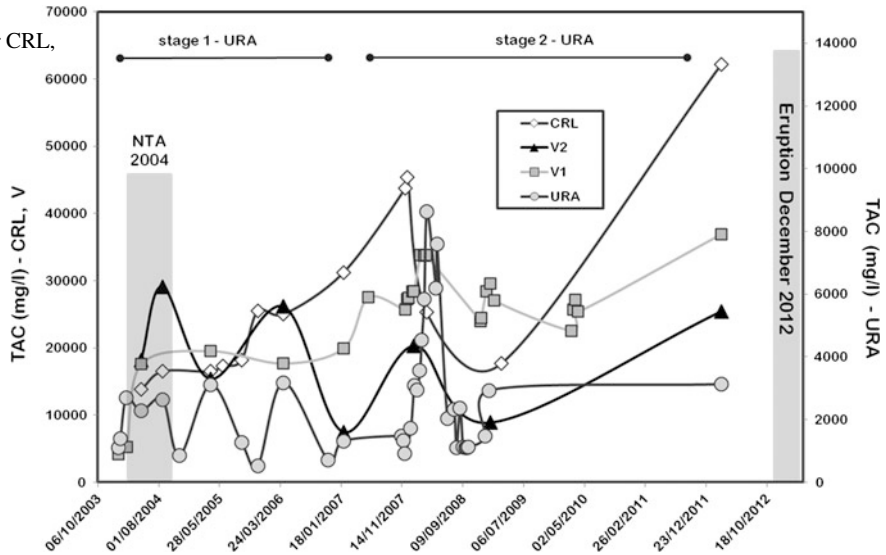
The total anion content (TAC) of CRL and V1 spring shows a temporal pattern for 2003–2012 consistent with that of lake surface temperature (Agosto et al. 2012). Lower TAC_{CRL} and TAC_{V1} values were observed during the NTA period and increase afterwards (Fig. 9.12). On the contrary, the V2 spring shows an opposite behavior:

TAC_{V2} is highest during the NTA period and decreases afterwards. This suggests that CRL and V1 were directly affected by the input of a hot SO_4 -Cl rich fluid, whereas the V2 spring had an independent fluid source for this period (Fig. 9.12). Saturation indices were determined for polymorphs of silica, gypsum and sulfur for the normal conditions of the crater lake (2005) and anomalous conditions in May and August 2004 (Fazio et al. 2008). For the NTA period, the crater lake waters were saturated or supersaturated in gypsum, quartz, cristobalite and amorphous silica. When normal conditions were reestablished in 2005, the crater lake only showed saturation in quartz and cristobalite.

Simultaneously, the URA water shows a period with a lower TAC (stage 1), and a second period with a higher TAC (stage 2) contemporary with increases in TAC in CRL and V1 (Fig. 9.12). During both stages, even with different TAC, the URA waters display seasonal behavior controlled by dilution processes. It shows the highest TAC in the dry summer, a lower TAC in correspondence with snowfall in winter, and lowest TAC during the snowmelt spring-summer period. Note that during the first stage, the URA shows a relatively constant seasonal pattern only disturbed during the NTA interval (Fig. 9.12).

Comparing the ionic groups (anions and cations) respect to major magmatic species (SO_4 ,

Fig. 9.12 Temporal variations in TAC for CRL, V1, V2 and URA



Cl, F) allows the identification of variations filtering the effects of seasonality and dilution by rainfall. They also indicate variations in the degassing regime of a magmatic system and in the water-rock interaction processes (Giggenbach and Glover 1975; Rowe et al. 1992a, b, Christenson and Wood 1993; Delmelle and Bernard 1994).

During the NTA interval, a negative excursion in Anions/SO₄ (mass) is documented for all members of the system (CRL, V springs and URA), indicating a relative increase in SO₄ compared to the rest of the anions in the waters (Fig. 9.13a). After the NTA interval, positive peaks occur in that ratio and then the whole system stabilizes with Anions/SO₄ at ~1.3–1.4. The positive peaks after the NTA interval indicate a relative increase of Cl and F. This alternation of peaks in ratios points out that during the NTA initially SO₄ enrichment occurred followed by a relative Cl and F increase. As observed during the 2000 eruption, the order of enrichment of magmatic species (anions) is consistent with the order of degassing of these species from a rising melt or a degassing fluid (Giggenbach 1996; Symonds et al. 2001; Aiuppa et al. 2002).

The anomalous behavior of the system during the NTA interval (2004) is associated with just a disturbance of the shallow hydrothermal environment, because no eruptive event occurred. High values of Cations/SO₄ (mass) were observed prior to, and a marked decrease during the NTA interval, stabilizing towards the end of the sampling period (Fig. 9.13b). The relatively high RFE concentrations suggest increased primary rock leaching before the NTA. During the NTA interval, Cations/SO₄ values decrease as a result of a marked increase in SO₄, and/or precipitation of secondary minerals, which involve both the leached material and fluids coming from deep environments. Towards the end of the high frequency sampling period (2009–2010), despite a significant increase in TAC (stage 2 in Fig. 9.12), the element ratios remained constant (Fig. 9.13a, b), indicating a stabilization of the system.

The changes in cation concentrations over time are best illustrated through fluctuations in the concentrations in the V1 spring. The element-time patterns do not change dramatically when normalized to Cl (Fig. 9.14), indicating that these variations are not simply dilution effects but true inputs and withdrawals in the major cation contents through W/R interaction and secondary

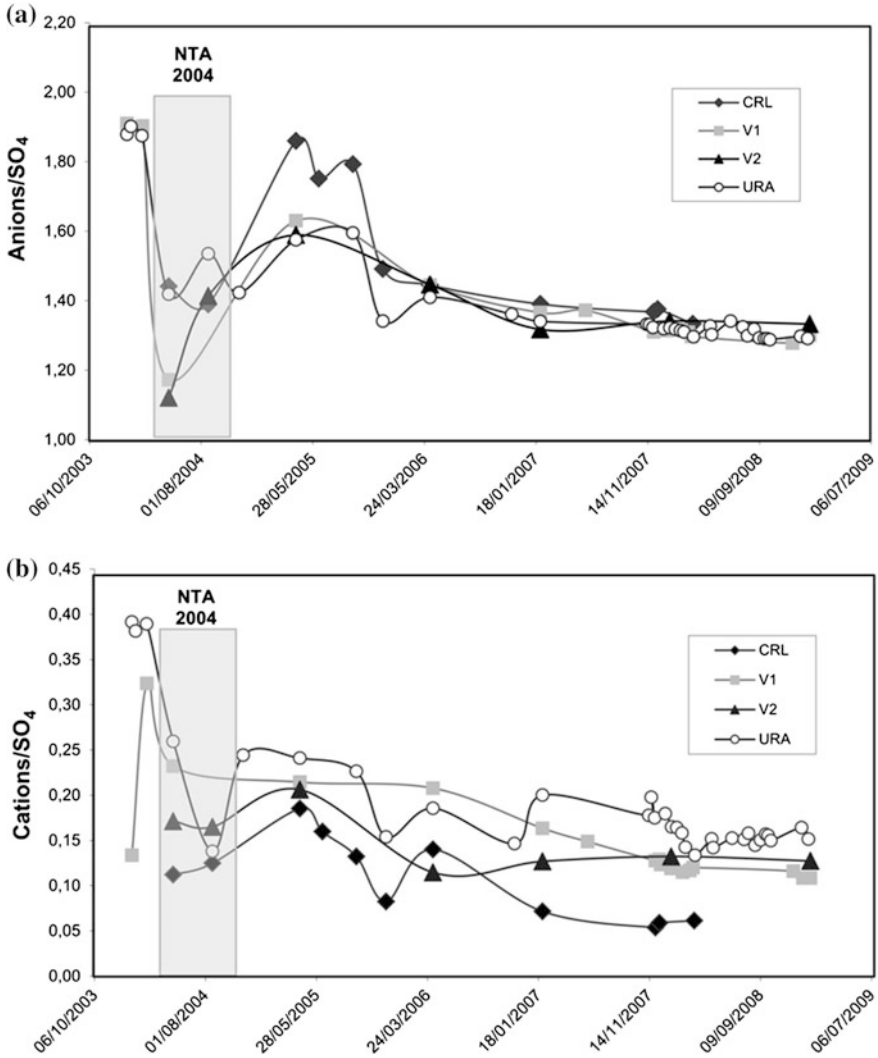
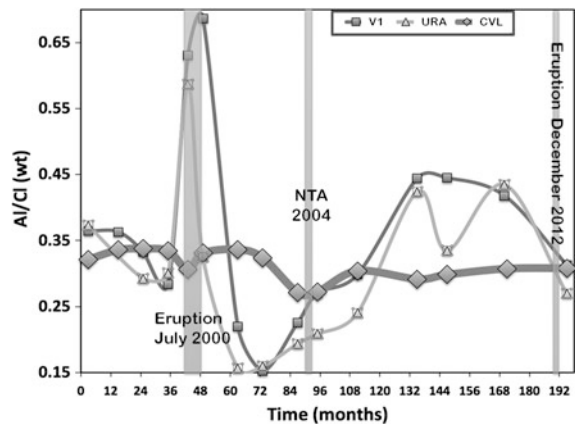


Fig. 9.13 Temporal variations in **a** Anions/SO₄ ratios, and **b** Cations/SO₄ ratios for CRL, V1, V2 and URA

Fig. 9.14 Al/Cl in the V spring, the URA and in a composite of Lake Cavihue profiles by year, showing the sharp drop after the 2000 eruption and the start of a drop after the 2012 eruption



mineral precipitation. The Al concentration in the springs and URA (and Al/Cl) drops precipitously after the 2000 eruption, which was related to the alunite crystallization in the hydrothermal reservoir. The K concentration versus time pattern is very similar.

The decrease in Al/Cl in Lake Caviahue is much more muted (Fig. 9.14), and lags those in the V spring and the URA. The large volume of CVL and its mixing properties cause these delayed responses (see below).

9.4.2 Variations in Chemistry of Lago Caviahue and the Lower Río Agrio

Lago Caviahue is a large volume (0.47 km³) glacial lake that is kept acidic by the URA effluents. The URA discharges in between the two arms of the lake, and at this time there is uncertainty towards the mixing behavior of these fluids with respect to depth and between the two lake arms. The river water may be colder than the lake water during the spring snow melting, and more concentrated and warmer during the hot summer. A plume of cold, dilute water may descend while mixing with the lake waters in spring and the more concentrated, but slightly warmer water in summer may also descend and mix. Despite these uncertainties, the data show only minor compositional differences between the southern and northern arm of the lake at a given time, and the vertical compositional gradients are small, so these waters do mix thoroughly over time. The lake is probably fully mixed during the winter season but is thermally stratified during the summer. The water residence time was estimated at 2.5 years by Rapacioli (1985) and at ~3.5–4.0 years by Varekamp (2003). The lake stratification negates the quantification of the mean whole-lake water residence times somewhat, but still, it indicates that the compositional variation of CVL will be lagging the compositional fluctuations in the URA. The composition of CVL is not a good aid in volcanic

surveillance, but provides a broad average of compositional trends over time without all the small compositional variations that the URA, CRL and V waters present (see above).

Secular trends in lake water composition from 1997–2006 capture the 2000 eruption and the 2004 NTA (Varekamp 2008). The compositional trends from 1997 to 2013 provide an extension of these earlier data. The pH of the lake decreased during and following the 2000 eruption, followed by a long period of relative dilution and gently increasing pH values. The pH crossed the value of 3 in 2009, but then became more acidic again in 2012, possibly prior to and after the 2012 eruption (Alexander 2014). The TDS shows a strong peak during the 2000 eruption and a small “bump” during the 2004 NTA. Overall, the lake became more dilute past 2004, but some elements started to increase again in 2006. Examples of time versus Cl, K and Mg concentrations are shown (Fig. 9.15), together with data from the Lower Río Agrio. The mean whole lake data show a smooth trend whereas the CVL depth profiles show more scatter as they probably represent different mixing events and inputs over time in the lake. The surface water samples (A series from Augusto et al. 2012) show more variation in Cl as a result of a higher frequency sampling and the local dilution controlled by the seasonal behavior, as observed for URA. The K concentrations of Augusto et al. (2012) are mostly higher whereas the Mg values are all lower than the Varekamp (2008) data, probably a consequence of the different sampling points and imperfect mixing of the lake, although some analytical variability in either data set cannot be totally excluded.

Most striking in the pattern is the very strong dilution that takes place after the 2000 eruption: the hydrothermal system almost ‘shut down’ in 2001, which was documented with strongly decreased element fluxes through the URA and dilution trends in the lake, especially for Al, Fe, K, and SO₄ (Varekamp 2008). The dilution in the lake could be the same for all elements if simply the discharge from the springs decreased. The

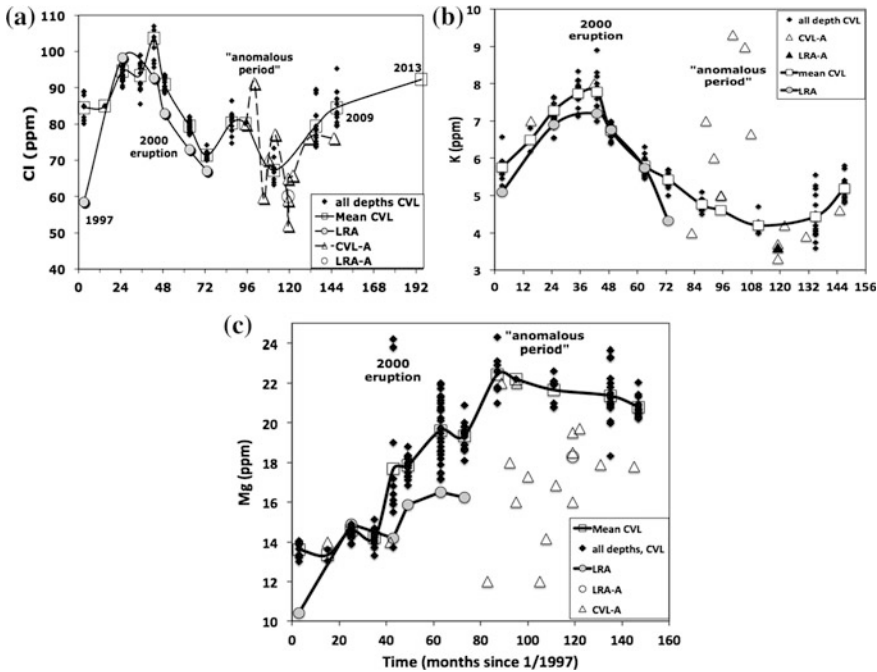


Fig. 9.15 Secular trends: **a** Trend of Cl concentration in CVL with build up to eruption followed by rapid drop off. Then again an increase during the 2004 NTA followed by a drop off and then a slow rise to 2013 values; **b** trend of K versus time, with sharp drop off after 2000 eruption and

minor to no effects during the NTA. Steep rise during the 2008–2009 period; **c** trend of Mg versus time, with an increase during the 2000 eruption but followed by a long term rise, with a slight decrease after the 2004 NTA

percentage drop was calculated from the 2000 high values for all elements and the following grouping appears: a 40–46 % drop for Cl, Al, Mg and Na whereas a bigger relative drop for K, Fe and SO₄ (56–66 %) is found. This is also shown in a 100 K/Cl versus time plot (Fig. 9.16),

indicating that after the eruption the 100 K/Cl value dropped from highs of 9 to 5.5–6, suggesting that K decreased more than Cl. The 100 K/Cl values of the A data series shows a close coherence with the other data, suggesting that local dilution effects in the surface waters

Fig. 9.16 Trend of 100 K/Cl over time, showing the drop off after the 2000 eruption and the strong decrease during the 2004 NTA. This is related to the saturation of alunite-jarosite in the hydrothermal cell below Copahue

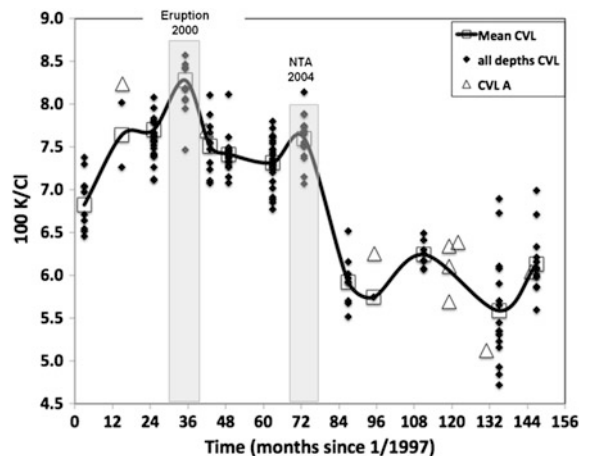


Fig. 9.17 Brown yellow Schwertmannite mineral precipitates in the riverbed near the Salto del Agrio (picture from J.C. Varekamp)



indeed played a role here. So the reduction in element fluxes into the lake is not just a diminished discharge of the V springs: also the composition of the springs changed, as discussed above in Sect. 4.1. During this period directly following the eruption, the V fluids were saturated with jarosite and alunite, and as a result the fluxes of Fe, Al, K and SO_4 diminished greatly. Assuming that the hydrothermal fluids had reacted extensively with freshly intruded plugs of new magma during the eruption, leading to higher cation contents in the fluids, a higher degree of neutralization, and oversaturation in a range of minerals. The resulting mineral precipitation reduced the permeability in the system considerably, diminishing the flow rate of the springs. The 2004 NTA saw an increase in some element fluxes but a total shut off of fluids into CRL, suggesting again a strong mineral precipitation event during early 2004, but this time localized in the upper part of the hydrothermal system. This may have been preceded by intrusions of stringers of new magma into the hydrothermal system (“failed eruptions” of Varekamp et al. 2009) or may have been just a rise of hyperconcentrated deep fluids generating a local perturbation into the shallow hydrothermal system (Agusto 2011; Vélez et al. 2011; Agusto et al. 2012).

The LRA is a diluted expression of the outflow of CVL as it receives water from small melt water streams along its course. It passes through a small water fall at the exit of the caldera (near

bridge) and then is joined by the Río Trolope, which discharges largely groundwater and melt-water, with some effluents from the Copahue village thermal areas. The rivers flow then jointly towards the large cascade of the Salto del Agrio and then further to join the Río Ñorquín and then south to Loncopue. The pH of the LRA was <3 before and during the 2000 eruption but then with the dilution of the lake the pH became close to 3.1–3.2 in the area of the confluence before the Salto. Around 2002–2003, the riverbed near the Salto del Agrio turned deep brown yellow from fresh mineral precipitates (Fig. 9.17). The riverbed further down to the confluence with the Río Ñorquín also became coated with similar ‘ocher’ materials. The front of mineral precipitation moved slowly upstream to very near the outlet of CVL and CVL itself became saturated with the ocher phases in 2008–2009 (Kading 2010). With the renewed acidification starting in 2011 or 2012, no more new yellow precipitates formed and the existing minerals started to dissolve again. In 2013, much of the LRA near the lake outlet had lost most of the precipitates that formed earlier. The expectation was that CVL itself would become fully saturated with the yellow mineral and would turn bright yellow-brown in 2011. The renewed acidification prevented a lake wide mineral precipitation event.

The yellow brown mineral consists of an organic slurry with small mineral particulates, suggesting the involvement of bacterial reactions

in its precipitation. Studies with Xray diffraction, SEM-EDX, reflectance spectroscopy and TEM indicated that the mineral is Schwertmannite ($\text{Fe}_8\text{O}_8(\text{SO}_4)(\text{OH})_6\text{H}_2\text{O}$), which is a strong adsorbent for the polyvalent oxyanions of As, P and V (and also may build these elements into its structure on the SO_4 site). The main driver for saturation of Schwertmannite in the Fe and SO_4 rich CVL and LRA fluids is the pH: when the pH exceeds 3, the mineral will start to precipitate (Kading 2010). The other mineral assemblage may be a mixture of goethite-ferrihydrite and Schwertmannite because the Fe/S values are slightly higher than the stoichiometric value of Schwertmannite alone (Kading 2010). The concentrations of P, As and V on the Schwertmannite are respectively 5700, 1040 and 1800 ppm. The bacterial species ferroxidans sp. oxidizes the Fe^{2+} in the water to Fe^{3+} , which may cycle in a diel pattern through photoreduction (Parker et al. 2008). The thick brown C_{org} -rich deposits just before the Salto del Agrio are hosting abundant green macroflora that flourish on this P-rich substrate. The N-C concentrations and stable isotope values of these organic-rich deposits are $\text{N} = 2.6 \%$, $\delta^{15}\text{N} = +7.7 \%$, $\text{C} = 31.3 \%$ and $\delta^{13}\text{C} = -21.1$, with a resulting C/N (weight) of 11.9. These analyses indicate a strong bacterial organic component in the mineral deposit, with debris of subaquatic vegetation (SAV). The bacterial chemosynthesis and the C3 photosynthesis pathway of the SAV yield the intermediate $\delta^{13}\text{C}$ value. The nitrogen possibly derived from the effluents of the sewage treatment plant of Cavihue that discharges into the lake. The dissolution of the Schwertmannite in the last few years is releasing the P and As again, possibly with harmful effects downstream. The confluence of the Lower Río Agrio and Río Ñorquín has whitish mineral precipitates, presumably Al-oxides, which may have influenced the REE patterns in the river (Gammons et al. 2005).

The chemical data of CVL waters show a general similarity with those of the URA fluids, but in detail, some differences exist, as shown above. The meltwater streams also have their impact on the chemical composition of CVL,

despite their high degree of dilution. The range of composition in the URA is greater than in the CRL and V fluids as a result of the contributions of several tributaries. The issue of in situ weathering of the bedrock in the URA that may contribute to the dissolved load and ultimately to the compositional evolution of CVL has not been researched in detail and remains a topic to be explored (e.g., van Hinsberg et al. 2010).

9.5 Element Fluxes from the Copahue Hydrothermal System

Element fluxes were measured annually over the last 15 years at the URA bridge in Cavihue and near the Mapuche settlement just above the cascades area of the URA. The LRA was monitored at the bridge near the exit from the caldera. The URA data (water composition multiplied by water discharge rate) provide a good quantitative insight into chemical discharges that enter Lago Cavihue, which were tested with non-steady state models for the lake (Varekamp et al. 2009). The general agreement between the evolution of the CVL composition and measured fluxes suggests that these annual measurements provide a first order quantification of element export rates from the hydrothermal system. From these element export rates, dissolved rock export rates, which are then recast into pore space created in the reservoir, were estimated. Detailed flux estimates for each element and their variation over time were presented by Varekamp et al. (2009). The total element export rate (in tonnes/month) shows variations over time (Fig. 9.18), with strong reductions in flux just after the 2000 eruption and with the 2004 NTA. This is true for both RFE and VE, and as argued before based on element concentrations, the VE flux is much larger than the RFE flux. The response to these flux variations is clearly reflected in the compositional trends of Lake Cavihue (Fig. 9.19), providing a coherent picture. The total RFE mass flux curve also shows a strong similarity with the %AW curve based on $\delta^{18}\text{O}$ in the V fluids

Fig. 9.18 Trend in the total mass fluxes into the lake for VE and RFE. Strong pulse during the 2000 eruption and drop off afterwards (shut down) with a smaller scale repeat during the 2004 NTA

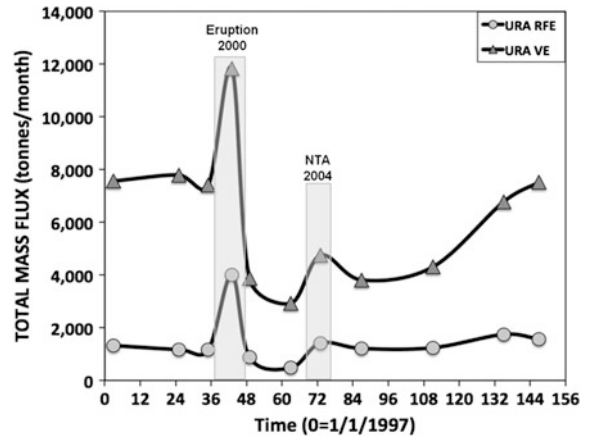
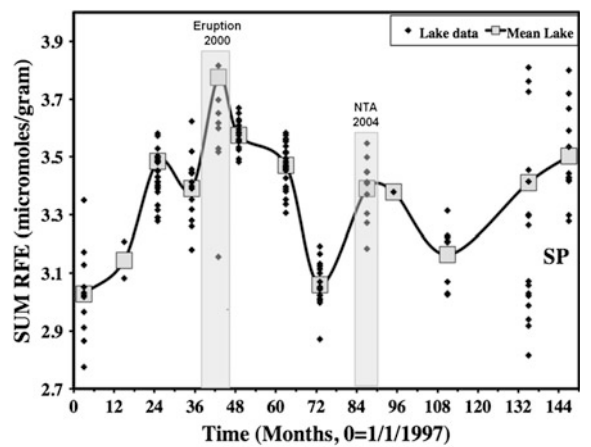


Fig. 9.19 Trend in the sum of the RFE against time, showing the 2000 eruption and 2004 NTA as positive excursions and a renewed increase in 2008–2009



(Fig. 9.9). When the hydrothermal component in the V fluids decreases, the measured fluxes in the URA decrease in a similar pattern.

The VE element export rate (Fig. 9.18) can be recast as an equivalent SO₂ flux (e.g., tonnes SO₂/day) which is the conventional parameter determined on passively degassing volcanoes that do not have a hydrothermal system that scrubs the magmatic volatiles. A mean of ~100 tonnes SO₂/day was exported as dissolved SO₄ through the Río Agrio over the main 12 year period of observation. Through the disproportionation reaction (Eq. 9.2), an additional fraction of magmatic sulfur is retained in the hydrothermal system as liquid sulfur and only emitted periodically as sulfur pyroclastics during phreatomagmatic events (e.g., 1992, 1995, 2000, 2012 eruptions). An estimate of this fraction,

using Eq. 9.2 is another 150 tonnes SO₂/day, for a mean total of 250 tonnes SO₂/day as the estimated magmatic sulfur flux. This is similar to many passively degassing volcanoes (<http://so.gsfc.nasa.gov>), but here none of that SO₂ reaches the atmosphere because all is scrubbed as SO₄ and SO (Symonds et al. 2001). In this calculation the precipitation of anhydrite has not been considered, but is considered relatively small because Ca does not show a significant offset in the iso sol diagram (Fig. 9.6).

The RFE fluxes are a measure of rock dissolution rates in the hydrothermal system. The mean rock removal rate, using Mg as a conservative index element together with an average of all Copahue rocks (Varekamp et al. 2004) as the rock protolith is about 11,000 tonnes rock/month. That value does not consider that a

significant fraction of the rock ($\sim 55\%$) is retained as hydrothermal silica. As a result, the net rock export rate is thus $\sim 5,000$ tonnes rock/month. This amount of rock is resupplied during the small intrusive events that occur periodically, as referred to earlier. The total amount of rock removed during the 12 year period of observation is $\sim 800,000$ tons, which would occupy a volume of about $300,000\text{ m}^3$ (at a density of 2.5 g/cm^3) that is equivalent to a 500 m deep hole with a 20 m diameter. Assuming the size of the hydrothermal system at $\sim 1\text{ km}^3$ (underlying the whole Copahue volcanic cone), the porosity or void space created by this dissolution process can be estimated. The ‘dissolution porosity’ is on the order of a few % in the 12 year period. This relatively small value suggests that other processes may create more permeability and porosity, such as seismic activity and associated faulting. The total amount of dissolved rock contained in Lago Cavihue is on the order of 160,000 tonnes (corrected for silica retention in the hydrothermal system).

Of interest is also the contents of nutrients and toxins in CVL (As and P, both largely derived from the hydrothermal system) and their associated in and outfluxes. On average, 1450 tonnes F, 6 tonnes As and 2 tonnes Li per year carried into Lake Cavihue, were measured, most of which leaves again through the Lower Río Agrío. Most of the As was locked up in the Schwertmannite beds in the LRA, but F and Li probably behaved close to conservative and were further transported downstream.

9.6 Events that Impacted the Hydrothermal System at Copahue Volcano

9.6.1 The 1993, 1995 and 2000 Eruptions

Volcanic activity at Copahue has been reported since the eighteenth century, but good documentation of activity started only with the eruptive cycle beginning July 1992. That cycle

continued into 1993, with major eruptions in December 1994 and September 1995. The crater lake explosions ejected hydrothermally altered rock fragments, siliceous white dust, copious amounts of green and yellow liquid sulfur and some basaltic-andesitic fragments (Delpino and Bermudez 1993, 1995). Unfortunately, no data were provided on the geochemistry of the hydrothermal fluids during this period. From 1997 to 2000, the Cl concentrations in the crater lake initially decreased, but during 1999 the concentrations and lake water temperatures increased considerably. By early 2000 the temperature of the CRL was extremely low ($5\text{--}8\text{ }^\circ\text{C}$), while the Vertientes springs remained at high temperatures ($70\text{--}75\text{ }^\circ\text{C}$). During July 2000 magmatic eruptions (VEI 1–2) occurred, starting with phreatomagmatic events and continuous degassing between eruptive phases until October 2000. Explosions ejected incandescent bombs and dark ash with chilled sulfur fragments covered an area up to 50 km from the crater (Global Volcano Network 2000a, b).

The RFE/Cl values and the ‘degree of neutralization’ (Varekamp et al. 2000) of the fluids declined in the crater lake and hot spring during the few years prior to 2000 eruption. Varekamp et al. (2001) suggested that this resulted from increased water/rock ratios in the hydrothermal system as a result of rock dissolution as well as that the rock protolith possibly became covered with liquid sulfur and/or cristobalite, slowing water-rock reaction. The REE patterns during this period showed enrichment in LREE relative to the rock. The degree of neutralization was $\sim 50\%$ but then decreased towards lower values by late 1999, possibly signaling enhanced volcanic gas inputs from rising magma.

The July 2000 fluids show a dramatic change, the RFE/Cl ratios increased, and RFE ratios in the fluids differed from those in the older Copahue rocks and in the 2000 magma. The 2000 intrusion of fresh magma into the hydrothermal system led to increased RFE/Cl values in the fluids, and water compositions became specially enriched in Mg. During the 2000 eruption, the hot spring fluids became more concentrated, the REE pattern became closer to that of the bulk rock, and the

fluxes of Mg, Na, Fe and Al increased strongly. The composition of these fluids resulted from the incongruent dissolution of the newly intruded magma with saturation of alunite, anhydrite, and silica phases at temperatures of 150 °C and up (Varekamp et al. 2009). The retention of these secondary phases may explain why the K, Al and Ca concentrations in the fluids have increased less than those of Fe, Mg, and Na.

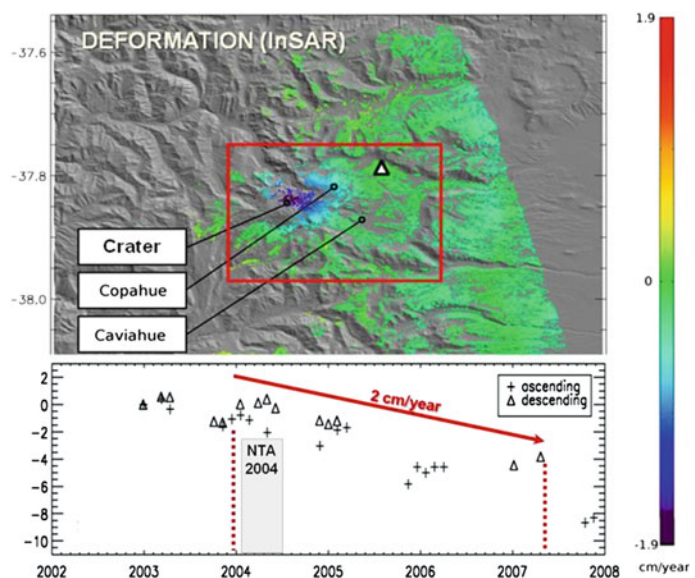
In the years following the 2000 eruption, strong variations in element ratios occurred, and the REE became heavily fractionated in both the HREE as well as the LREE. The negative Eu anomaly in the pre-eruptive fluids decreased in magnitude (Eu/Eu^* increased) during the 2000 eruption and in late 2004, suggestive of preferential plagioclase dissolution in the fluids.

9.6.2 The 2004 NTA Event

The temperature of the CRL waters decreased in early 2004, reaching 13 °C in May 2004. By July 2004, ~80 % of the lake surface was frozen probably for the first time (Fig. 9.3), while hot springs displayed high water temperatures: 81 °C_{V1} and 69 °C_{V2}. During the NTA, the

Anions/SO₄ ratio indicated initially a relative SO₄ enrichment followed by a relative Cl and F increase. The V2 showed an increase in TAC, while TAC_{CRL} and TAC_{V1} showed the lowest values at that time (Fig. 9.12). The temperature and TAC decrease in CRL, and simultaneous increase in V2, suggest that a decrease in the mass and heat flux occurred in the shallow part of the underlying hydrothermal system (Agusto 2011). Saturation indices of the lake water during the NTA increased for gypsum, quartz, cristobalite and amorphous silica (Fazio et al. 2008), probably the result of the arrival of a hyperconcentrated deep fluid that cooled in the shallow part of the hydrothermal system. Most likely, hydrothermal inputs into the lake ceased temporarily during the NTA as a result of partial sealing of the upper conduit and crater floor below the lake due to mineral precipitation in the fractures (Agusto et al. 2012). The permeability of the upper reaches of the hydrothermal system also may have been influenced by increased viscosity of molten sulfur present there. The viscosity of liquid sulfur increases at temperatures 150–250 °C (Oppenheimer 1992; Takano et al. 1994a, b) and a viscous cap of sulfur may have partly isolated the lake from uprising magmatic fluids

Fig. 9.20 Deflation of the Copahue volcano: **a** mean velocity deformation map 2002–2008; **b** deformation temporal serie volcano summit showing 2 cm/year subsidence since 2004. Start of deflation volcano during NTA interval



(Takano et al. 1994a, b; Delmelle et al. 2000; Christenson et al. 2010), which would be an additional explanation for the frozen lake at that time.

Deflation (negative surface deformation) was also observed since early 2004 on the Copahue volcanic edifice, with a maximum subsidence rate of 2 cm/year (Fig. 9.20; Vélez et al. 2011). Analytical models indicated that the source of deformation was located at ~ 4 km depth below the volcanic edifice, with an estimated decrease in volume of $0.0015 \text{ km}^3/\text{year}$ (Vélez et al. this book). Deflation processes on volcanoes are sometimes associated with the release of magmatic brines from the plastic to the brittle zone (Fournier 2006), resulting in strong degassing through the conduit toward surface. Such a process could have caused a release of hot and concentrated deep fluids into the shallow Copahue volcanic-hydrothermal system, leading to: (i) increased TAC in the V springs and URA, (ii) secondary mineral precipitations in fractures below the crater lake, (iii) increased temperature of the molten sulfur increasing the viscosity, and thus (iv) decreased permeability in the upper part of the system ultimately leading to the freezing over of the lake (Agosto et al. 2012). The increased element export fluxes during 2004 (Varekamp et al. 2009) may support the contention that a small magmatic intrusion could have been involved as well (“failed eruption?”), although the deflation of the volcanic edifice can not be explained by such an event alone.

By the end of 2004 the crater lake icy surface melted again (Fig. 9.3), and during the following years (2005–2010) it had temperatures between 30 and 40 °C, while the outlet temperature of the two hot springs had dropped and remained relatively constant ($T_{V1} = 60\text{--}70$ °C, and $T_{V2} = 40\text{--}50$ °C). Between 2005 and 2011, the crater lake had no significant changes in temperature, and water level. On the other hand, the concentrations of anions related to the input of magmatic gases increased progressively.

9.7 Changes Affecting the Crater Volcanic-Hydrothermal System Related to the 2012 Eruption

Phreatic and phreatomagmatic eruptions occurred in 2012 after 12 years of a solfataric state. A column of water vapour and acidic gases was observed some 200–300 m above the crater in November–December 2011, indicating an increased fluid discharge rate from the volcano summit. By March 2012, the waters from the hot springs and crater lake showed (1) the highest acidity ($\text{pH} < 0$), (2) high temperatures (~ 65 °C), (3) highest contents of magmatic VE species (SO_4^{2-} , Cl^- , F^-) since the 2000 eruption (Fig. 9.12), and (4) a significant decrease of the crater lake water level due to enhanced evaporation (Agosto et al. 2013a).

A phreatic eruption occurred on July 17, manifested by vertical jets 10 m above the crater lake level. On July 19, a minor phreatomagmatic event occurred with the expulsion of pyroclastic material. During the following months, fumarolic activity and intense bubbling continued, the crater lake waters remained at high temperatures ($\sim 60^\circ$), with high acidity ($\text{pH} < 0$), and extremely high electrical conductivity. The lake water level continued to decrease until becoming a boiling pool only ~ 20 m in diameter just before the December 2012 eruption.

A bigger phreatomagmatic eruption occurred on December 22nd (Caselli et al. this book). Chilled liquid sulfur was recognized in the erupted pyroclastic material, suggesting the presence of molten sulfur at the lake bottom or below in the hydrothermal system. As the eruption continued, the last remnants of the crater lake disappeared, the hot springs were covered by a pyroclastic surge, and the course of the URA was modified. High temperature fumaroles and liquid sulfur ponds formed inside the crater. The maximum measured fumarole temperature (420 °C) was close to the local boiling temperature of liquid sulfur (440 °C) (Agosto et al. 2013a). Two

months later, the crater lake began to reform and in March–April 2013, two water pools with intense gas bubbling were observed. During the 12 years prior to the 2012 eruption, the frequency of sampling monitoring of Copahue acidic waters (CRL, V and URA) had decreased, and not much chemical water data is available.

9.8 Conceptual Model of the Copahue Crater Volcanic-Hydrothermal System

The wealth of chemical and physical data presented above has led to a conceptual model for Copahue crater and its hydrothermal system (Fig. 9.21). Prior to and during eruptions, stringers of new magma intrude into the hydrothermal system, creating a higher pressure and temperature, and therefore a higher flow rate of the V springs and CRL input. This then is accompanied by an increase in magmatic VE species like SO_4 and Cl. The fresh rock protolith reacts with the hot acid fluids which become enriched in RFE (symbolized by e.g., much higher Mg). The fluids then evolve towards secondary mineral saturation involving sulfate bearing minerals like jarosite, alunite, anhydrite/gypsum and hydrothermal silica. The

precipitation of these minerals reduces the porosity and permeability of the upper part of the system, and the formation of liquid sulfur leads to the filling of pore spaces and vents (Fig. 9.21b). This reduction in permeability after an intrusive event or eruptive period, leads to strongly reduced fluxes of all elements (reduced permeability-reduced flow rates) and especially reduced fluxes of K-Al-Fe (jarosite-alunite retention), as observed after the 2000 eruption and after the 2004 NTA. The latter was not associated with an eruption, but probably as result of an input of deep magmatic fluids and/or a small magmatic intrusion. This event caused precipitation of minerals in the high part of the system, cutting off the pathways to the crater lake which then froze over. The flow rates of the springs may have first increased (increased element fluxes) but then also decreased when further mineral precipitation reduced permeability in the system. The recovery of the system may be that with ongoing “flushing” through the system of magmatic volatiles and exhaustion of the protolith, the secondary minerals start to dissolve again (enhanced TAC and Al-K-Fe fluxes) as seen in 2008–2009, creating new permeability and enhanced fluid flow (Figs. 9.12 and 9.17).

The sealing of fractures that vent into the crater lake decreases the intensity of convection in the lake. The lake may form an incipient stratification,

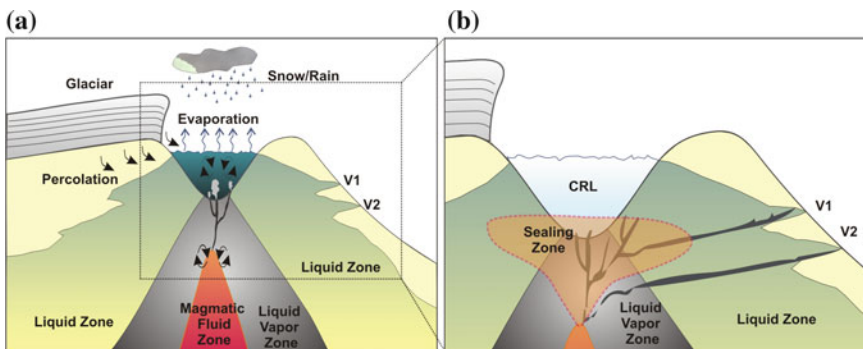


Fig. 9.21 Conceptual model for fluid circulation patterns at the Copahue crater: **a** Indication of the area affected by permeability changes in the fractures that feed the upper volcanic-hydrothermal system, physical steady-state situation: open fracture system and free movement of fluids

prior to NTA period; **b** decreased permeability by fracture sealing that feed Cr and V1 during NTA period, generating the lake freezing and reduced salinity of Cr and V1 waters, channeling the flow of deep origin through V2

with warmer concentrated bottom waters affected by hydrothermal inflow, and cooler but more dilute surface waters exposed to the low atmospheric temperatures. Lake water color changes and variations in turbidity may indicate these variations in degree of stratification (Delmelle and Bernard 2000a). The combined effect of decreased heat input into the lake, with enhanced stratification may have led to the frozen lake water surface during the NTA in July 2004 (Agosto 2011).

A drop in permeability by the filling of fractures results in a gradual pressure increase in the shallow volcano-hydrothermal system. Decompression can occur through (1) a sudden pressure release through a phreatic explosion (the 1992 and 1995 phreatic eruptions), or (2) a more gradual pressure release by changes in the fluid circulation in the summit system (post-NTA period) (Agosto et al. 2012). The return to “normal” degassing then reestablishes the convective mechanism in the lake leading to thermal and compositional homogenization, manifested in the crater lake by its more normal appearance (Fig. 9.21a).

The permeability decrease of the upper part of the system, by partial or complete sealing of fractures may control the phreatic eruption dynamics. When the pressure buildup in the shallow volcanic-hydrothermal system reaches a critical value, and the decompression process does not take place by fluid drainage through flank springs, phreatic explosions are necessary to relieve the excess pressure in the summit volcanic-hydrothermal system, as occurred between 1992 and 1995.

This hypothesis is consistent with the composition of pyroclastic material ejected during the 1992 and 1995 phreatic explosions (Delpino and Bermúdez 1993, 1995) and the hydrothermally altered fragments involved in 2000 and 2012 eruptions (Delpino and Bermúdez 2002; Caselli et al. this book). In addition, the 1992 phreatic eruptions González Ferrán (1995) indicated that explosions also took place through a smaller crater outside the lake-bearing crater. This suggests that the sealing effect can become so efficient that the pressure release took place adjacent to the main volcanic duct.

9.9 Recommendations for Monitoring of Volcanic Activity at Copahue Volcano

During the last two decades, a discontinuous geochemical sampling program was carried out by various investigators on effluent waters of the Copahue volcanic-hydrothermal system. The available compiled geochemical data provide several new insights into the behavior of this system and make suggestions for improved volcanic surveillance. The Copahue crater lake is a typical example of a hyperacidic lake whose water composition may serve as a direct sensor for the hydrothermal and possibly eruptive activity of the underlying volcanic system. Traditional geochemical monitoring (e.g., SO₂ flux monitoring) is not feasible at Copahue due to the absence of summit fumaroles and the occurrence of the well-developed hydrothermal aquifer below the crater where magmatic gases are almost completely scrubbed. On the contrary, URA is a very suitable place for volcano monitoring due to its easy access throughout the year (including the winter period) and its direct relationship with the water coming downslope from the volcano that impact the RFE and VE contents as observed during the 2000 eruption (Figs. 9.11 and 9.16). The URA at the “bridge of Caviahue” (Fig. 9.1) has been most frequently sampled for waters associated with the volcanic-hydrothermal system. The URA is sensitive to seasonal changes because of inputs of snowmelt waters and rain but its seasonal behavior is predictable and reasonably well known. Temporal variations of major RFE cation contents (Fig. 9.22a) follow the seasonal pattern. Compositional variations in the magmatic-hydrothermal system are easily detected as significant deviations from the seasonal trends in the river.

Compositional variations superposed on seasonal trends were particularly noticeable during the 2004 NTA interval (Fig. 9.22). The contents of K, Mg and Al deviated from the seasonal pattern, with higher values than expected during high rainfall periods (AIC 2007). Minor elements such as Mn and B (Agosto 2011) also increased

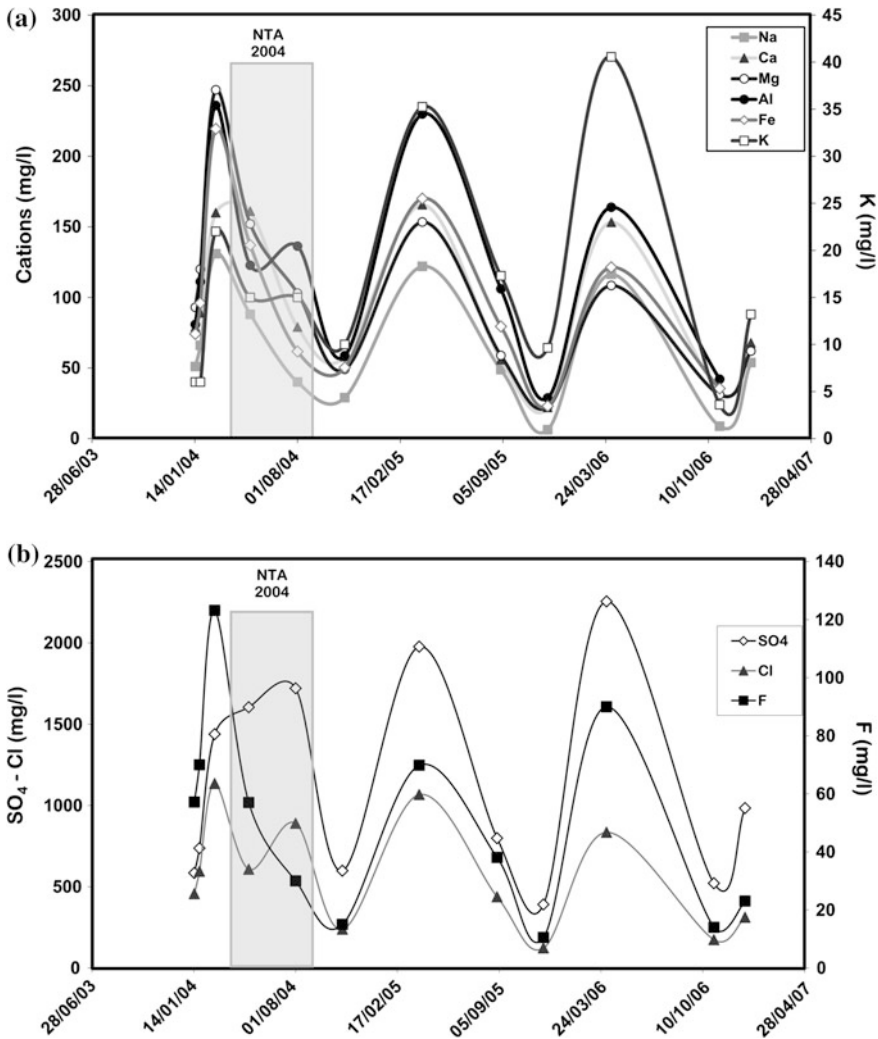


Fig. 9.22 Temporal variations in URA waters: **a** RFE, elements in mg/l; **b** aions in mg/l

at that time, suggesting enhanced hydrothermal effluxes from the system. Boron is enriched in magmatic fluids and behaves conservatively (Tonani 1970; Palmer et al. 1987; Martini 1989; Tassi et al. 2005, 2009), and an increase in B concentrations indicates a pulse of concentrated deep fluids that is transported to the surface and emitted into the URA. The increased B values were associated with enhanced VE concentrations during the NTA, with an especially sharp increase in SO₄ values, followed by Cl and to a lesser extent F (Fig. 9.21b).

SO₄/Cl, Mg/Cl and Mg/SO₄ values would make suitable indicators of disturbance

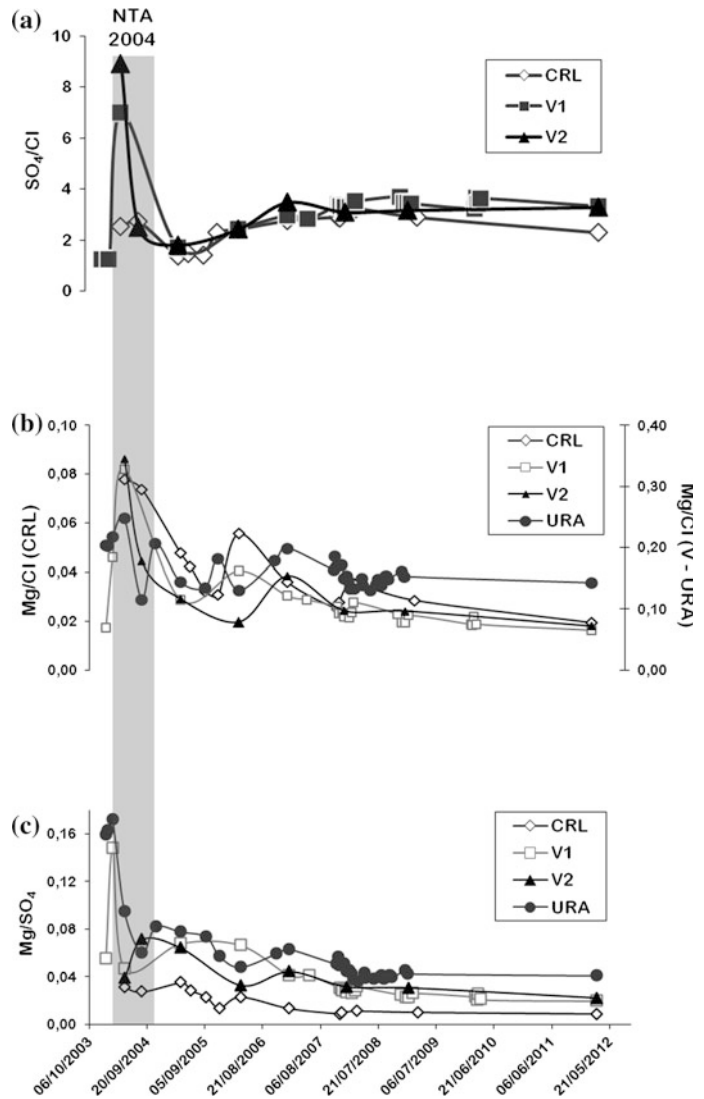
(precursors?) in the volcanic-hydrothermal environment: enhanced releases of deep hydrothermal fluids to the surface and/or enhanced water-rock interaction. An increase in SO₄/Cl ratio was observed in the system during the 2000 eruption (Fig. 9.11; Varekamp et al. 2009) which may have been related to an intrusion of new magma in the system with degassing of deep fluid during ascent. The lower solubility of SO₂ with respect to HCl in magmas may make the SO₄/Cl value a useful indicator for rising magma batches (Martini 1993; Giggenbach 1996).

The Mg/Cl ratio is a parameter widely applied in geochemical monitoring of active crater lakes

(Giggenbach 1974; Christenson 2000; Ohba et al. 2008; Tassi et al. 2009; Christenson et al. 2010; Rouwet and Tassi 2011). This ratio showed a rapid increase during the eruption of 2000, particularly in the URA (Varekamp et al. 2004). An increase in Mg/Cl in the crater lake environment can also indicate increased loss of HCl by evaporation from the lake surface (Rowe et al. 1992a; Christenson and Wood 1993; Delmelle and Bernard 2000a, b; Rouwet and Ohba 2015), making the lake environment less suitable for this parameter.

Varekamp et al. (2006) identified a less negative Eu anomaly and a correlation between the LREE enrichment pattern of erupted rocks and waters from the 2000 eruptive period, and during 2004. Accordingly, the authors explained these observations by intrusions of small magma stringers into the volcanic-hydrothermal system, with preferential dissolution of plagioclase in the early stages. These intrusions then continued with the 2000 phreatomagmatic eruption. The Eu anomaly variation during the NTA of 2004 was not followed by an eruption (“failed eruption”,

Fig. 9.23 Temporal variations CRL, V and URA waters: **a** SO₄/Cl ratio; **b** Mg/Cl ratio; **c** Mg/SO₄ ratio



Varekamp et al. 2009), but provided evidence for a perturbation of the hydrothermal system (Agusto 2011). The enhanced SO_4/Cl and Mg/Cl values prior to the NTA interval (Fig. 9.23a,b) were excellent precursors of “hydrothermal perturbation” (Agusto et al. 2012). The SO_4/Cl seems to be a more effective predictor in V1 and V2 than in the CRL and URA, while Mg/Cl is also significant in the CRL, and Mg/SO_4 clearly indicated the upcoming NTA in the URA and V springs (Fig. 9.23c). The Al/Cl parameter may be useful to signal the beginning of the ‘plugging’ of the hydrothermal system and heralding a period of post-eruptive activity following an active period (Fig. 9.14).

In conclusion, the establishment of a small monitoring post with regular sample collection at the bridge of the URA at Caviahue would be the most efficient mode of starting a regular volcano monitoring program at Copahue volcano.

References

- Agusto M (2011) Estudio geoquímico de los fluidos volcánicos e hidrotermales del Complejo Volcánico Copahue Caviahue y su aplicación para tareas de seguimiento. Ph.D. Thesis, Buenos Aires, Argentina, Universidad de Buenos Aires, pp 294
- Agusto M, Tassi F, Caselli A, Vaselli O, Rouwet D, Capaccioni B, Chiodini G (2013a) Thermal and chemical changes in the crater lake of Copahue volcano (Argentina) prior to the December 2012 phreatomagmatic eruption. IAVCEI General Assembly 2013, Kagoshima Japan, pp 1019
- Agusto M, Tassi F, Caselli A, Vaselli O, Rouwet D, Capaccioni B, Caliro S, Chiodini G, Darrah T (2013b) Gas geochemistry of the magmatic-hydrothermal fluid reservoir in the Copahue-Caviahue Volcanic Complex (Argentina). *J Volcanol Geoth Res* 257:44–56
- Agusto M, Tassi F, Caselli A, Vaselli O, dos Santos Afonso M (2012) Seguimiento geoquímico de las aguas ácidas del sistema volcán Copahue – Río Agrio: posible aplicación para la identificación de precursores eruptivos. *Rev As Geol Arg* 69(4):481–495
- Aiuppa A, Federico C, Paonita A, Pecoraino G, Valenza M (2002) S, Cl and F degassing as an indicator of volcanic dynamics: the 2001 eruption of Mount Etna. *Geophys Res Lett* 29. doi: [10.1029/2002GL015032](https://doi.org/10.1029/2002GL015032)
- Alexander E (2014) Aqueous geochemistry of an active magmato-hydrothermal system: Copahue Volcano, Río Agrio, and Lake Caviahue, Neuquén, Argentina. BA Thesis Middletown, CT USA, Wesleyan University, pp 100
- AIC (2007) Autoridad Interjurisdiccional de las Cuencas de los ríos Limay, Neuquén y Negro. Datos meteorológicos de la región de Caviahue entre los años 2003 y 2007. Cipolletti, Río Negro, Informe Inédito, pp. 5
- Barnes JD, Sharp ZD, Fischer TP (2009) Variations in chlorine stable isotopes along the Central American volcanic front. *Geochem Geophys Geosys* 7:Q08015. doi:[10.1029/2009GC002587](https://doi.org/10.1029/2009GC002587)
- Bermudez A, Delpino D (1995) Mapa de los peligros potenciales en el área del Volcán Copahue – sector Argentino. Volcanic Hazard Map. The Geological Survey of the Province of Neuquen, Argentina
- Boschetti T (2013) Oxygen isotope equilibrium in sulfate–water systems: a revision of geothermometric applications in low-enthalpy systems. *J Geochem Explor* 124:92–100
- Bowen GJ, Revenaugh J (2003) Interpolating the isotopic composition of modern meteoric precipitation. *Water Resour Res* 39(10):1299. doi:[10.129/2003WR002086](https://doi.org/10.129/2003WR002086)
- Brown G, Rymer H, Dowden J, Kapadia P, Stevenson D, Barquero J, Morales LD (1989) Energy budget analysis for Poás crater lake: implications for predicting volcanic activity. *Nature* 339:370–373
- Caselli A, Agusto M, Fazio A (2005) Cambios térmicos y geoquímicos del lago craterico del volcán Copahue (Neuquén): posibles variaciones cíclicas del sistema volcánico. XVI Congreso Geológico Argentino, La Plata, Argentina, pp 751–756
- Caselli A, Vélez ML, Agusto M, Forte P, Albite J, Daga R (2013) Erupción del volcán Copahue (Argentina): evolución, productos e impacto social y ambiental. Foro Internacional sobre Peligros Geológicos, Arequipa, Peru, pp 104–109
- Christenson BW (2000) Geochemistry of fluids associated with the 1995–1996 eruption of Mt. Ruapehu, New Zealand: signatures and processes in the magmatic hydrothermal system. *J Volcanol Geoth Res* 97:1–30
- Christenson BW, Wood CP (1993) Evolution of a vent-hosted hydrothermal system beneath Ruapehu Crater Lake, New Zealand. *Bull Volcanol* 55:47–565
- Christenson BW, Werner CA, Reyes AG, Sherburn S, Scott BJ, Miller C, Rosenberg MJ, Hurst AW, Britten K (2007) Hazards from hydrothermally sealed volcanic conduits. *EOS* 88(50):53–55
- Christenson BW, Reyes AG, Young R, Moebis A, Sherburn S, Cole-Baker J, Britten K (2010) Cyclic processes and factors leading to phreatic eruption events: Insights from the 25 September 2007 eruption through Ruapehu Crater Lake, New Zealand. *J Volcanol Geoth Res* 191:15–32
- Craig H (1961) Isotopic variations in meteoric waters. *Science* 133:1702–1703
- Craig H, Gordon LI, Horibe Y (1963) Isotopic exchange effects in the evaporation of water. *J Geophys Res* 68:5079–5087
- Cronin SJ, Hodgson KA, Neall VE, Palmer AS, Lecointre JA (1997) 1995 Ruapehu lahars in relation

- to the late Holocene lahars of Whangaehu River. New Zealand. *NZ J. Geol Geophys* 40:507–520
- Delmelle P, Bernard A (1994) Geochemistry, mineralogy, and chemical modeling of the acid crater lake of Kawah Ijen Volcano, Indonesia. *Geochim Cosmochim Acta* 58(11):2445–2460
- Delmelle P, Bernard A (2000a) Volcanic lakes. *Encyclopedia of Volcanology*. Academic Press, pp 877–896
- Delmelle P, Bernard A (2000b) Downstream composition changes of acidic volcanic waters discharged into the Banyupahit stream, Ijen caldera, Indonesia. *J Volcanol Geoth Res* 97:55–75
- Delmelle P, Bernard A, Kusakabe M, Fisher TP, Takano B (2000) Geochemistry of the magmatic hydrothermal system of Kawah Ijen volcano, east Java, Indonesia. *J Volcanol Geoth Res* 97:31–53
- Delpino D, Bermudez A (1993) La Actividad del Volcan Copahue durante 1992: Erupcion con emisiones de azufre piroclastico, Provincia del Neuquen, Argentina. XII Congreso Geologico Argentino, Mendoza, Argentina, pp 292–301
- Delpino D, Bermúdez A (1995) Eruptions of pyroclastic sulfur at crater lake of Copahue Volcano, Argentina. *International Union of Geodesy and Geophysics. XXI General Assembly, Boulder, USA*, pp 128
- Delpino DH, Bermudez AM (2002) La erupción del volcán Copahue del año 2000. Impacto social y al medio natural. Provincia del Neuquen, Argentina. XV Congreso Geologico Argentina, El Calafate, Argentina
- Eggenkamp HG, Middelburg J, Kreulen R (1994) Preferential diffusion of ^{35}Cl relative to ^{37}Cl in sediments of Kau Bay, Halmahera, Indonesia. *Chem Geol* 116:317–325
- Fazio A, Agosto M, Farías S, Caselli A (2008) Evaluación de posibles fases minerales en equilibrio en el sistema volcánico Copahue (Neuquén) y su vinculación con parámetros químicos. XVII Congreso Geológico Argentino. Jujuy, Argentina, pp 1343–1344
- Fehn U, Peters E, Tullai-Fitzpatrick S, Kubik P, Sharma P, Teng R, Gove H, Elmore D (1992) 129I and 36Cl concentrations in waters of the eastern Clear Lake area, California: residence times and source ages of hydrothermal fluids. *Geochim Cosmochim Acta* 56:2069–2079
- Fehn U, Snyder G, Varekamp JC (2002) Detection of recycled marine sediment components in crater lake fluids using ^{129}I . *J Volcanol Geoth Res* 115:451–460
- Fournier RO (2006) Hydrothermal systems and volcano geochemistry. In: Dzurisin D (ed) *Volcano deformation*. Springer, Berlin, pp 153–194
- Gammons C, Wood S, Pedrozo F, Varekamp J, Nelson B, Shope C, Baffico G (2005) Hydrogeochemistry and rare earth element behavior in a volcanically acidified watershed in Patagonia, Argentina. *Chem Geol* 222:249–267
- Gat JR (1995) Stable isotopes of fresh and saline lakes. In: Lerman A, Imboden D, Gat J (eds) *Physics and chemistry of lakes*. Springer, Berlin, pp 139–165
- Gat JR, Levy Y (1978) Isotope hydrology of inland sabkhas in the Bardawil area, Sinai. *Limnol Oceanogr* 23(5):841–850
- Gibson JJ, Edwards TW, Prowse TD (1999) Pan-derived isotopic composition of water vapour and its variability in northern Canada. *J Hydrol* 217:55–74
- Giggenbach WF (1974) The chemistry of Crater Lake, Mt. Ruapehu (New Zealand) during and after the 1971 active period. *NZ J Sci* 17:33–45
- Giggenbach WF (1987) Redox processes governing the chemistry of fumarolic gas discharges from White Island, New Zealand. *Appl Geochem* 2:143–161
- Giggenbach WF (1996) Chemical composition of volcanic gases. In: Scarpa WF, Tilling (eds) *Monitoring and mitigation of Volcano Hazards*. Springer, Berlin, pp 222–256
- Giggenbach WF, Glover RB (1975) The use of chemical indicators in the surveillance of volcanic activity affecting the crater lake on Mt. Ruapehu. *NZ Bull Volcanol* 39:70–81
- Giggenbach WF, Corrales Soto R (1992) Isotopic and chemical composition of water and steam discharges from volcanic-magmatic-hydrothermal systems of the Guanacaste geothermal province, Costa Rica. *Appl Geochem* 7:309–332
- GVN (2000a) Frequent Ash explosions and acidic mudflows starting on July 1. *Bull Global Volcano Netw* 25:6
- GVN (2000b) Continued ash explosions and tremor during August–October. *Bull of Global Volcano Netw* 25:9
- Healy J, Lloyd EF, Banwell CJ, Adams RD (1965) Volcanic eruption on Raoul Island, November 1964. *Nature* 205:743–745
- Kading T (2010) Natural pollutant attenuation by schwertmannite at Copahue Volcano, Argentina. M.A. Thesis, Wesleyan University, Middletown, CT, USA, p 247
- Kusakabe M, Komoda Y, Takano B, Abiko T (2000) Sulfur isotope effects in the disproportionation reaction of sulfur dioxide in hydrothermal fluids: implications for the $\delta^{34}\text{S}$ variations of dissolved bisulfate and elemental sulfur from active crater lakes. *J Volcanol Geoth Res* 97:287–308
- Liebscher A, Barnes JD, Sharp ZD (2006) Chlorine isotope vapor–liquid fractionation during experimental fluid-phase separation at 400 C/23 MPa to 450 C/42 MPa. *Chem Geol* 234:340–345
- Martini M (1989) The forecasting significance of chemical indicator in areas of quiescent volcanism: examples from Vulcano and Phlegrean Fields (Italy). In: Latter JH (ed) *Volcanic hazard*. Springer, Berlin, pp 372–383
- Martini M (1993) Gases Volcánicos. In: Martí J, Araña V (eds) *La volcanología actual. Nuevas Tendencias*. Consejo Superior de Investigaciones Científicas, España, pp 387–444
- Martini M, Giannini L, Buccianti A, Prati F, Cellini Legittimo P, Iozzelli P, Capaccioni B (1991) 1980–

- 1990: ten years of geochemical investigation at Phelegrean Fields (Italy). *J Volcanol Geoth Res* 48:161–171
- Mas L, Mas G, Bengochea L (2000) Heatflow of Copahue geothermal field, its relation with tectonic scheme. In: *Proceedings of world geothermal congress, Tohoku, Japan*, pp 1419–1424
- Mayr C, Lu A, Stichler W, Trimborn P, Ercolano B, Oliva G, Ohlendorf C, Soto J, Fey M, Haberzettl T, Janssen S, Scha F, Schleser GH, Wille M, Zolitschka (2007) Precipitation origin and evaporation of lakes in semi-arid Patagonia (Argentina) inferred from stable isotopes ($\delta^{18}\text{O}$, $\delta^2\text{H}$). *J Hydrol* 334:53–63
- Morrissey M, Gisler G, Weaver R, Gittings M (2010) Numerical model of crater lake eruptions. *Bull Volcanol* 72:1169–1178
- Naranjo JA, Polanco E (2004) The 2000 AD eruption of Copahue Volcano, Southern Andes. *Rev Geol Chile* 31(2):279–292
- Ohba T, Hirabayashi J, Nogami K (2008) Temporal changes in the chemistry of lake water within Yugama Crater, Kusatsu-Shirane Volcano, Japan: implications for the evolution of the magmatic-hydrothermal system. *J Volcanol Geoth Res* 178:131–144
- Oppenheimer C (1992) Sulphur eruptions at Volcán Poás, Costa Rica. *J Volcanol Geoth Res* 49:1–21
- Ouimette AP (2000) Hydrothermal processes at an active volcano, Copahue, Argentina. M.A. Thesis, Wesleyan University, Middletown, CT, USA, pp 220
- Palmer MR, Spivack AJ, Edmond JM (1987) Temperature and pH controls over isotopic fractionation during adsorption of boron on marine clays. *Geochim Cosmochim Acta* 51:2319–2323
- Panarello HO (2002) Características isotópicas y termodinámicas de reservorio del campo geotérmico Copahue-Caviahue, provincia del Neuquén. *Rev As Geol Arg* 57(2):182–194
- Parker S, Gammons C, Pedrozo F, Wood S (2008) Diel changes in metal concentrations in a geogenically acidic river: Rio Agrio, Argentina. *J Volcanol Geoth Res* 178:213–223
- Pasternack G, Varekamp J (1997) Volcanic lake systematics I. Physical constraints. *Bull Volcanol* 58:528–538
- Pedrozo F, Temporetti P, Beamud G, Diaz M (2008) Volcanic nutrient inputs and trophic state of Lake Caviahue, Patagonia, Argentina. *J Volcanol Geoth Res* 178:205–212
- Rapacioli R (1985) Lake Caviahue and its basin. Tech. Report, EPAS Gov. Office, Province of Neuquen, Argentina, pp. 1–72
- Rouwet D, Ohba T (2015) Isotope fractionation and HCl partitioning during evaporative degassing from active crater lakes. In: Rouwet D, Christenson BW, Tassi F, Vandemeulebrouck J (eds) *Volcanic lakes*. Springer, Heidelberg, pp 179–200
- Rouwet D, Tassi F (2011) Geochemical monitoring of volcanic lakes. A generalized box model for active crater lake. *Ann Geophys* 54(2):161–173
- Rowe GL Jr, Brantley SL, Fernandez M, Fernandez JF, Borgia A, Barquero J (1992a) Fluid-volcano interaction in an active stratovolcano: the crater lake system of Poás volcano, Costa Rica. *J Volcanol Geoth. Res* 49:23–51
- Rowe GL Jr, Ohsawa S, Takano B, Brantley SL, Fernandez JF, Barquero J (1992b) Using crater lake chemistry to predict volcanic activity at Poás volcano, Costa Rica. *Bull Volcanol* 54:494–503
- Seal RR, Alpers CN, Rye RO (2000) Stable isotope systematics of sulfate minerals. In: Alpers CN, Jambor JL, Nordstrom DK (eds) *Sulfate minerals—crystallography: geochemistry and environmental significance*, pp 541–602
- Sharp ZD, Barnes JD, Brearley AJ, Chaussidon M, Fischer TP, Kamenetsky VS (2007) Chlorine isotope homogeneity of the mantle, crust and carbonaceous chondrites. *Nature* 446:1062–1065
- Stoibert J, Rose W (1970) The geochemistry of Central-American volcanic gas condensates. *Geol Soc Amer Bull* 81:2891–2912
- Symonds RB, Gerlach TM, Reed MH (2001) Magmatic gas scrubbing: implications for volcano monitoring. *J Volcanol Geoth Res* 108:303–341
- Takano B, Watanuki K (1989) Monitoring of volcanic eruptions at Yugama crater lake by aqueous sulfur oxyanions. *J Volcanol Geoth Res* 40:71–87
- Takano B, Ohsawa S, Glover RB (1994a) Surveillance of Ruapehu Crater Lake, New Zealand, by aqueous polythionates. *J Volcanol Geoth Res* 60:29–57
- Takano B, Saitoh H, Takano E (1994b) Geochemical implications of subaqueous molten at Yugama crater lake, Kusatsu-Shirane volcano, Japan. *Geochem J* 28:199–216
- Taran YA, Pokrovsky BG, Dubik YM (1989) Isotopic composition and origin of water from andesitic magmas. *Dokl (Trans) Ac Sci USSR* 304:440–443
- Tassi F, Vaselli O, Capaccioni B, Giolito C, Duarte E, Fernández E, Minissale A, Magro G (2005) The hydrothermal-volcanic system of Rincon de la Vieja volcano (Costa Rica): a combined (inorganic and organic) geochemical approach to understanding the origin of the fluid discharges and its possible application to volcanic surveillance. *J Volcanol Geoth Res* 148:315–333
- Tassi F, Vaselli O, Fernández E, Duarte E, Martínez M, Delgado-Huertas A, Bergamaschi F (2009) Morphological and geochemical features of crater lakes in Costa Rica: an overview. *J Limnol* 68(2):193–205
- Tonani F (1970) Geochemical methods of exploration for geothermal energy. *Geothermics* 2:492–515
- van Hinsberg V, Berlo K, Sumarti S, van Bergen M, Williams-Jones E (2010) Extreme alteration by hyperacidic brines at Kawah Ijen volcano, East Java, Indonesia: II Metasomatic imprint and element fluxes. *J Volcanol Geoth Res* 196:169–184
- Varekamp J (2003) Lake contamination models: evolution towards steady state in stratified lakes. *J Limnol* 62 (1):67–72
- Varekamp J (2008) The acidification of glacial Lake Caviahue, Province of Neuquen, Argentina. *J Volcanol Geoth Res* 178:184–196

- Varekamp JC, Kreulen R (2000) The stable isotope geochemistry of volcanic lakes: examples from Indonesia. *J Volcanol Geoth Res* 97:309–327
- Varekamp J, Pasternack G, Rowe G (2000) Volcanic lake systematics. II. chemical constraints. *J Volcanol Geotherm Res* 97:161–179
- Varekamp J, Ouimette A, Herman S, Bermudez A, Delpino D (2001) Hydrothermal element fluxes from Copahue, Argentina: a “beehive” volcano in turmoil. *Geology* 29:1059–1062
- Varekamp J, Ouimette A, Kreulen R (2004) The magmato-hydrothermal system of Copahue volcano, Argentina. In: Wanty RB, Seal II RB (eds) *Water–rock interaction 11*, vol 1. Balkema Publishers, Leiden, pp 215–218
- Varekamp J, Maarten de Moor J, Merrill M, Colvin A, Goss A, Vroon P, Hilton D (2006) The geochemistry and isotopic characteristics of the Caviahue Copahue volcanic complex, Province of Neuquen, Argentina. *Geol Soc Am* 407:317–342
- Varekamp J, Ouimette A, Herman S, Flynn K, Bermudez A, Delpino D (2009) Naturally acid waters from Copahue volcano, Argentina. *Appl. Geochem* 24:208–220
- Varekamp J (2015) The chemical composition and evolution of volcanic lakes. In: Rouwet D, Christenson BW, Tassi F, Vandemeulebrouck J (eds) *Volcanic lakes*. Springer, Heidelberg, pp 93–123
- Vaselli O, Tassi F, Duarte E, Fernández E, Poreda R, Delgado-Huertas A (2010) Evolution of fluid geochemistry at the Turrialba volcano (Costa Rica) from 1998 to 2008. *Bull Volcanol* 72:397–410
- Velez ML, Euillades P, Caselli A, Blanco M, Martinez Diaz J (2011) Deformation of Copahue volcano: inversion of InSAR data using a genetic algorithm. *J. Volcanol. Geoth. Res* 202:117–126
- White WM (2013) *Geochemistry*. Oxford, UK, Blackwell-Wiley, p 672